University of Alberta

Mathematical Modeling of Visbreaking

by

Atul Saxena

A thesis submitted to the Faculty of Graduate Studies and Research
in partial fulfillment of the requirements for the degree of

Master of Science

in

Chemical Engineering

Department of Chemical and Materials Engineering

Edmonton, Alberta
Spring 2008

Library and Archives Canada

Published Heritage Branch

395 Wellington Street
Ottawa ON K1A 0N4
Canada

Bibliothèque et Archives Canada

Direction du Patrimoine de l'édition

395, rue Wellington
Ottawa ON K1A 0N4
Canada

Your file Votre référence
ISBN: 978-0-494-47636-9
Our file Notre référence
ISBN: 978-0-494-47636-9

NOTICE:
The author has granted a non-exclusive license allowing Library and Archives Canada to reproduce, publish, archive, preserve, conserve, communicate to the public by telecommunication or on the Internet, loan, distribute and sell theses worldwide, for commercial or non-commercial purposes, in microform, paper, electronic and/or any other formats.

The author retains copyright ownership and moral rights in this thesis. Neither the thesis nor substantial extracts from it may be printed or otherwise reproduced without the author's permission.

AVIS:
L'auteur a accordé une licence non exclusive permettant à la Bibliothèque et Archives Canada de reproduire, publier, archiver, sauvegarder, conserver, transmettre au public par télécommunication ou par l'Internet, prêter, distribuer et vendre des thèses partout dans le monde, à des fins commerciales ou autres, sur support microforme, papier, électronique et/ou autres formats.

L'auteur conserve la propriété du droit d'auteur et des droits moraux qui protège cette thèse. Ni la thèse ni des extraits substantiels de celle-ci ne doivent être imprimés ou autrement reproduits sans son autorisation.

In compliance with the Canadian Privacy Act some supporting forms may have been removed from this thesis.

While these forms may be included in the document page count, their removal does not represent any loss of content from the thesis.

Conformément à la loi canadienne sur la protection de la vie privée, quelques formulaires secondaires ont été enlevés de cette thèse.

Bien que ces formulaires aient inclus dans la pagination, il n'y aura aucun contenu manquant.

Canada

To the loving memory of my father..

...

Abstract

Previously, nuclear magnetic resonance (NMR) carbon-type analysis data were used to model visbreaking of Athabasca bitumen [1], where the major reaction pathways during visbreaking were identified. The present work extends the same approach further to explain the visbreaking behavior of six different oils.

In the current study, the visbreaking of these oils was performed at a single severity and the feed and the products were separated into different pseudo-components. The quantification of carbon-types in these pseudo-components was done using elemental analyses and nuclear magnetic resonance spectroscopy. Four classes of representative model compounds were chosen based on the carbon-type data of the pseudo-components. A literature review of the pyrolysis studies of these model compounds suggested the major types of reactions involved during visbreaking. Through the use of reaction pathways and model rules, model correlations were able to predict the residue conversion, coke formation and product yields during visbreaking.

Acknowledgements

I would like to extend my thanks to my supervisors Dr. Carolina Diaz-Goano and Dr. Heather Dettman for their guidance, support and encouragement throughout my graduate program and research. This thesis would not have been possible without their dedicated efforts. I would like to thank my other professors at the University of Alberta for their able guidance and scholarship. I would also extend my gratitude to my friends and fellow scholars at the Department of Chemical and Materials Engineering for their assistance during my graduate program. This research was supported by the Natural Sciences and Engineering Research Council (NSERC), the Department of Chemical and Materials Engineering at the University of Alberta, the National Centre for Upgrading Technology (NCUT) through partial funding by the Canadian Program for Energy Research and Development (PERD), the Alberta Research Council and the Alberta Energy Research Institute. As well, I would wish to acknowledge Dr. David Patmore and the NCUT Highhead Group for performing the autoclave runs; Ms. Allison Ross and Ms. Sara Salmon for analysis coordination, quality control and preparing the SARA fractions, and the NCUT Analytical Group for performing the distillations and analyses. And lastly, I thank my wife, Shweta, whose unflinching love and support has always spurred me to act on my dreams.

Table of Contents

1 Introduction 1
- 1.1 Modeling of Hydrocarbon Conversion Processes . . . 2
- 1.2 Research Objective . . . 3
- 1.3 Thesis Overview . . . 3

2 Background Concepts: A Review 4
- 2.1 Visbreaking Process and its Types . . . 4
  - 2.1.1 Soaker Visbreaking . . . 5
  - 2.1.2 Coil Visbreaking . . . 6
- 2.2 Visbreaking Severity and its Constraints . . . 7
  - 2.2.1 Coke Formation . . . 9
  - 2.2.2 Fuel Stability . . . 10
- 2.3 Previous Work on Visbreaking Kinetic Models . . . 11
- 2.4 Carbon-types . . . 14
  - 2.4.1 Role of Nuclear Magnetic Resonance (NMR) Spectroscopy in Quantification of Carbon-types . . . 18
- 2.5 Thermal Cracking Mechanism . . . 18
  - 2.5.1 Initiation . . . 20
  - 2.5.2 Propagation . . . 21
  - 2.5.3 Termination . . . 21
  - 2.5.4 Structure-Reactivity Relationships . . . 22

3 Experimental Work 25
- 3.1 Experimental Visbreaking Conditions . . . 25
- 3.2 Fraction Preparation . . . 26
- 3.3 Characterization of Pseudo-components . . . 26
  - 3.3.1 Gas Analysis . . . 26
  - 3.3.2 Elemental Analysis . . . 26
  - 3.3.3 Coke Content . . . 27
  - 3.3.4 Nuclear Magnetic Resonance Spectroscopy . . . 27

4 Model Data and Approach 29
- 4.1 Model Data . . . 29
  - 4.1.1 Pseudo-component Content in Feed and Product . . . 29
  - 4.1.2 Gas Component Analysis . . . 29
  - 4.1.3 Elemental Analysis . . . 31
  - 4.1.4 Coke Yield . . . 31
  - 4.1.5 NMR Carbon-type Analysis . . . 32
- 4.2 Model Approach . . . 32
  - 4.2.1 NMR Carbon-type Analysis . . . 32
  - 4.2.2 Residue Conversion . . . 35

4.2.3 Coke Formation and Carbon-types 37
4.2.4 Representative Model Compounds 38
4.2.5 Major Reactions during Visbreaking 48

5 Model Development and Results **50**
5.1 Model Development 50
5.1.1 Residue Conversion 50
5.1.2 Coke Formation 51
5.1.3 Reaction Pathways 54
5.1.4 Model rules 58
5.1.5 Product Correlations for Gas Formation 60
5.1.6 Product Correlations for Naphtha Formation 64
5.1.7 Prediction of Gasoil and Residue Formation 70

6 Model Use and Validation **73**
6.1 Model Use 73
6.2 Model Validation 74

7 Conclusions and Future Work **76**
7.1 Conclusions 76
7.2 Future Work 78

Bibliography **79**

Appendix **85**

A List of Product Gases **85**
A.1 Product Gases 85

B Error Analysis **86**
B.1 Error Analysis 86

C Sample Calculations **88**
C.1 Sample Calculations for Athabasca Bitumen 88

List of Tables

2.1 Activation Energy in kcal/mol 20
A.1 Complete List of Product Gases 85

List of Figures

2.1 Reaction Rate Constant for Visbreaking [7] 6
2.2 Soaker Visbreaking Process [9] 7
2.3 Coil Visbreaking Process [9] 8
2.4 C-C Bond Dissociation Energy [28] 15
2.5 C-H Bond Dissociation Energy [28] 16
2.6 Bond Energies for 2-Dodecyl-9,10-dihydrophenanthrene [29] 17
2.7 BDEs of Aryl Radicals of Six Different Groups of PAHs [30] 17
2.8 NMR Carbon-types 19
2.9 PPN Pyrolysis Pathways [40] 21
2.10 PPN Pyrolysis Mechanism [40] 22
2.11 Empirical Structure-Reactivity Relationship for Saturated Cyclic Compounds [44] 23
2.12 Mechanistic Structure-Reactivity Relationship for Saturated Cyclic Compounds [45] 24

4.1 Pseudo-component Content in Feed and Product 30
4.2 Gas Component Analysis 30
4.3 Elemental Analysis 31
4.4 Coke Yield 32
4.5 NMR Carbon-type Analysis for Athabasca Bitumen 33
4.6 Chemical Nature of Different Oils 34
4.7 Fraction of Chain Ends in Residue 35
4.8 Change in Residue after Visbreaking 36
4.9 Residue Conversion vs. Asphaltene Content of Feed 37
4.10 Residue Conversion vs. Aromatic Content of Feed 38
4.11 Percentage Conversion of Different Residue Pseudo-components 39
4.12 MCR vs. Aromatic Carbon Content [17] 39
4.13 Visbreaking Coke vs. Feed MCR 40
4.14 Visbreaking Coke vs. Feed Asphaltene 40
4.15 Percentage Conversion of Model Compounds [29] [49] [40] [43] [50] [51] 42
4.16 Effect of Chain length on Alkylpyrene Conversion [42] 43
4.17 Pyrolysis Pathways for DDP [49] 44
4.18 Pyrolysis Pathways for TDC [50] 44
4.19 Pyrolysis Pathways for DPP [43] 45
4.20 Pyrolysis Pathways for BPP [40] 46
4.21 Pyrolysis Pathways for DDPh [29] 47
4.22 Pyrolysis Pathways for 2ET [50] 48

5.1 Residue Conversion vs RRI 52
5.2 CCR vs Carbon-types 53
5.3 Visbreaking Coke vs. Carbon-types 53
5.4 Weighting Factors for Methane Formation 61

5.5 Carbon moles in CH4 vs Weighted sum of model parameters 62
5.6 Weighting Factors for C2 Formation 63
5.7 Carbon moles in C_2 vs Weighted sum of model parameters 63
5.8 Weighting Factors for C_3+ Formation 64
5.9 Carbon moles in C_3+ vs Weighted sum of model parameters 65
5.10 Weighting Factors for Naphtha Aromatics Formation 66
5.11 Product Naphtha aromatics vs Weighted sum of model parameters . . 67
5.12 Weighting Factors for Naphtha Cycloparaffins Formation 68
5.13 Product Naphtha Cycloparaffins vs Weighted sum of model parameters 69
5.14 Weighting Factors for Naphtha paraffins Formation 71
5.15 Product Naphtha paraffins vs Weighted sum of model parameters . . . 72

6.1 Model Predictions 75

List of Symbols

AFGOAr Athabasca Feed Gasoil Aromatics

AFGOP Athabasca Feed Gasoil Polars

AFGOS Athabasca Feed Gasoil Saturates

AFN Athabasca Feed Naphtha

AFRAr Athabasca Feed Residue Aromatics

AFRAs Athabasca Feed Residue Asphaltenes

AFRP Athabasca Feed Residue Polars

AFRS Athabasca Feed Residue Saturates

Ar Aromatic

As Asphaltene

BP Boiling Point

Br Branched

C-C Carbon-Carbon

C-H Carbon-Hydrogen

Cy Cycloparaffin

GO Gasoil

GOA Gasoil Aromatics

GOAr Gasoil Aromatics

GOP Gasoil Polars

GOS Gasoil Saturate

H/C Hydrogen to Carbon

IBP Initial Boiling Point

N	Naphtha
O	Olefin
P	Paraffin
R	Residue
RA	Residue Aromatics
RAr	Residue Aromatics
RAs	Residue Asphaltenes
RP	Residue Polars
RS	Residue Saturates
S	Sulfide

Chapter 1

Introduction

Thermal conversion is one of the primary processing technologies used for the upgrading of petroleum feedstock all over the world. It accounts for approximately 58 percent of worldwide installed capacity for residue upgrading. The other technologies used are hydroconversion and residue fluid catalytic cracking (RFCC). The two thermal conversion technologies used commercially include coking and visbreaking [2]. Coking units, which include delayed coking, fluid coking and Flexicoking have been on the rise worldwide because of a shift to heavy and sour crude oils [3]. However, with more than 150 units operating around the world, visbreaking still accounts for more than a quarter of the residue upgrading capacity of the world [2] [4].

Fuel oil is approximately 18 percent of the petroleum products worldwide [5]. Production of stable fuel oil with maximum viscosity reduction is the process objective of a typical visbreaker unit. The run-length of the unit is decreased by coke formation in the furnace coils and the soaker drum. Therefore, the main aim is to operate the unit with maximum conversion and minimum coking. Through mild thermal cracking, which lowers the viscosity of the heavy distillates and reduces the cutterstock demand for viscosity cutting of the fuel oil product, visbreaking increases the net distillate yield of the refinery. All this is achieved at a much lower cost than other residue upgrading processes like RFCC or hydroconversion that require high catalyst and high hydrogen consumption, respectively. Thus, it is the simplicity of a visbreaker unit that makes this technology the mainstay of many petroleum refineries. Visbreaking is the mildest and the least complex of the thermal cracking

technologies. Therefore it is the logical first step in the direction of studying and modeling of the thermal cracking process.

1.1 Modeling of Hydrocarbon Conversion Processes

Process models today are an inexpensive off-line and on-line tool used for process unit optimization, research and development, and making future investment decisions and are indispensable to modern business. A present-day process unit model is a combination of different blocks, that represent different equipment in a process unit and is used to predict product properties, product yields, fractionation efficiency, reactor pressure and temperature profiles, catalyst deactivation and coke formation in a unit. Advances in computation, refining chemistry analytical techniques and chemical kinetics have enabled a modern process model to make accurate hydrodynamic and kinetic predictions. However, modeling of physical and chemical processes of petroleum fractions is very challenging given the fact that the petroleum fractions host thousands of true chemical compounds that cannot be identified completely and whose information of chemical kinetics and chemical and physical properties is not available. Strict environmental regulations, deteriorating feed quality and the need to remain profitable have severely constrained the operation of a modern refinery. Present-day process models are expected to predict results in greater detail at a molecular level with a high level of accuracy. Not only are they expected to predict accurate yields but also the impurities in different process streams and the operational constraints faced with processing of different feeds, so that the refiner can encash the opportunity of processing a low-cost feed.

A process model is either empirical or mechanistic. An empirical model is based on collection of data and its mathematical correlation is based on minimal knowledge of the underlying physical and chemical principles. A mechanistic model is based primarily on the reaction chemistry and physical principles of the true chemical compounds or the pseudocomponents. Therefore a mechanistic model has better prediction capabilities than an empirical model but it is very expensive in terms of time and effort involved.

1.2 Research Objective

Previously, nuclear magnetic resonance (NMR) carbon-type analysis data were used to develop a mathematical model of mild thermal conversion (visbreaking) of Athabasca bitumen, where the major reaction pathways followed during visbreaking were identified. This approach has been extended in the current research to model the visbreaking behavior of six petroleum oils from different geographical locations around the world. In particular, the objective of this research is to advance the understanding of chemistry involved during visbreaking process by proposing rule-based correlations, based on feed carbon type data and the visbreaking reaction pathways, for predicting product(gas and liquid)yields, percentage residue conversion and coke formation during visbreaking at a single severity.

1.3 Thesis Overview

The rest of the thesis is organized as follows:

Chapter 2 discusses the visbreaking process and its types, visbreaking severity and constraints faced, NMR carbon-type analysis, thermal cracking reaction mechanism, and reviews existing visbreaker kinetic models.

Chapter 3 describes the experimental conditions for visbreaking and the analytical methods used for feed and product characterization.

Chapter 4 presents and discusses the experimental results. It also includes discussion on different classes of representative model compounds and their reactivity at experimental conditions where the main reactions during visbreaking are indicated.

Chapter 5 proposes different correlations for product yields, residue conversion and coke formation during visbreaking and for coke formation during severe thermal cracking process. The correlations are based on reaction pathways and model rules. Chapter 6 discusses model validation and its use.

Chapter 7 discusses the conclusions and possible future work from this research.

Chapter 2

Background Concepts: A Review

This chapter presents a review of the background concepts required for the analysis of thermal reactivity of different heavy oils. These concepts cover a wide spectrum from the process knowledge of visbreaking to the operational constraints faced and from the chemistry of heavy oils to thermal cracking mechanisms. A discussion on the existing visbreaking kinetic models is also included.

2.1 Visbreaking Process and its Types

The history of thermal cracking dates back to 1913 when William Burton was awarded the patent for thermal cracking of gasoil to gasoline. This process doubled the gasoline production from crude oil and thus helped meet the demands of a burgeoning automobile industry [6]. The thermal conversion process of gasoil to gasoline peaked in 1930 after which it was replaced by catalytic cracking for the production of gasoline [7]. Visbreaking or the viscosity breaking process of the heavy petroleum residue, was one of the many variants of the thermal cracking process developed between 1930 and 1940 [8]. Visbreaking is a once-through, mild conversion, liquid-phase thermal cracking process used primarily for the reduction of viscosity of the atmospheric residues, vacuum residues, asphalts and other heavy oils. These heavy oils, after cutter stock addition for subsequent viscosity reduction, are sold as fuel oil. After visbreaking, the demand for the cutter stocks for viscosity reduction

significantly decreases and this helps increase the distillate yield of a refinery. Apart from the cutter stock reduction, the production of gas and naphtha from a visbreaker is a secondary benefit. Due to higher demand for fuel oil in Europe and Asia, there is more visbreaking capacity in the world outside the US and Canada [2].

The conversion in a visbreaker can be defined in many different ways. It can be defined as the percentage of gas and gasoline produced, or the decrease in the amount of residue, or the decrease in the viscosity of residue, or the increase in specific gravity. Visbreaking, like thermal cracking, follows first-order kinetics. The first order rate equation for visbreaking, as given by Speight [7] is:

$$k = \frac{1}{t} \log\left(\frac{100}{X}\right) \tag{2.1}$$

where k is the first order reaction rate constant (s^{-1}), t is the reactor residence time in seconds and X is 900°F+ visbroken residuum yield in volume%. Figure 2.1 shows the visbreaking kinetic constant as a function of the coil outlet temperature. There are two types of commercial visbreaking process, Soaker and Coil visbreaking.

2.1.1 Soaker Visbreaking

In soaker visbreaking, the feed is preheated and then charged to a furnace with a coil outlet temperature of approximately 450°C. The onset of cracking takes place in the furnace after which the furnace effluent is fed to a soaker drum which operates at pressure between 7-15 kg/cm^2 with a defined residence time. Most of the thermal cracking takes place in the soaker vessel and the soaker effluent is then quenched and fractionated under atmospheric and vacuum conditions. In contrast to the old soaker vessels, which were down-flow in design and had coking problems, the new soaker vessels are mostly up-flow in design and are provided with perforated plates as internals to prevent back-mixing of the liquid flow [9]. The main operating variables in soaker visbreaking are the furnace temperature and the soaker pressure which govern the residence time in the soaker and the amount of cracking.

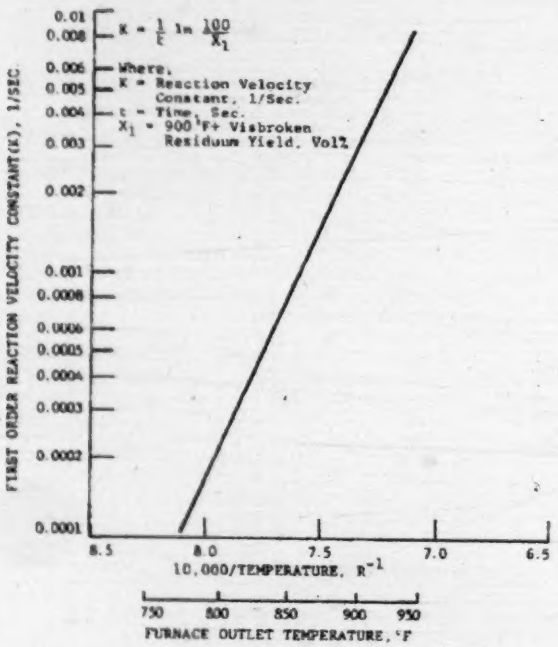

Figure 2.1: Reaction Rate Constant for Visbreaking [7]

2.1.2 Coil Visbreaking

In coil visbreaking, the feed after preheating is fed to a furnace, which operates at a coil outlet temperature higher than that of the soaker visbreaker furnace by about 30-50°C. All the cracking takes place in the coils of the furnace. The furnace effluent is then quenched, after which it is fractionated. The main operating variable is the coil outlet temperature which governs the extent of cracking. Due to the higher furnace temperature, the fuel costs are higher than the soaker visbreaker, though the additional fuel consumed is made up by the product heat recovery and the extra steam generation in the coil visbreaker.

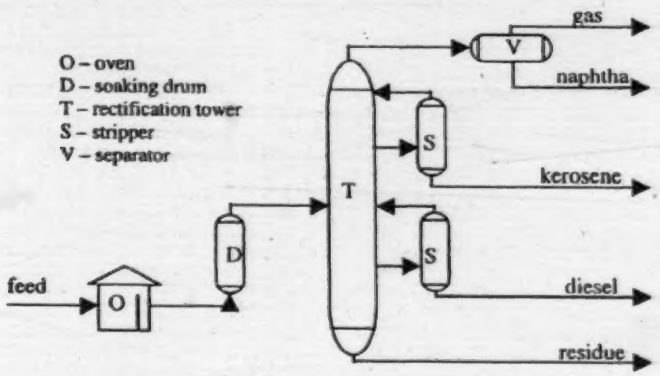

Figure 2.2: Soaker Visbreaking Process [9]

2.2 Visbreaking Severity and its Constraints

The cracking severity during visbreaking is defined in terms of severity factor which can be related to the product yields. In commercial units, the Soaking Volume Factor (SVF) is used to represent the process conditions like the residence time, temperature and pressure. The SVF is the ratio of the equivalent coil volume in cubic feet to the total visbreaker feed in bbl per day and is calculated at the base conditions of 750 psi and and 800°F [10]. The total SVF term has contributions from both the furnace coil and the soaker vessel.

$$\text{Total SVF} = \text{SVF}_{coil} + \text{SVF}_{drum} \tag{2.2}$$

$$\text{SVF}_{coil} = \frac{1}{F}\int_0^V RK_P dV \tag{2.3}$$

where F= total feed in bbl/day, R= ratio of the rate constant at reaction temperature to the rate constant at 800°F, K_P= pressure correction factor for pressure other than 750 psig, dV= incremental coil volume, and V= total coil volume.

$$\text{SVF}_{drum} = DVK_{TD}K_P/F \tag{2.4}$$

where DV= volume of the drum in ft^3, K_{TD}= reaction velocity constant at the mean

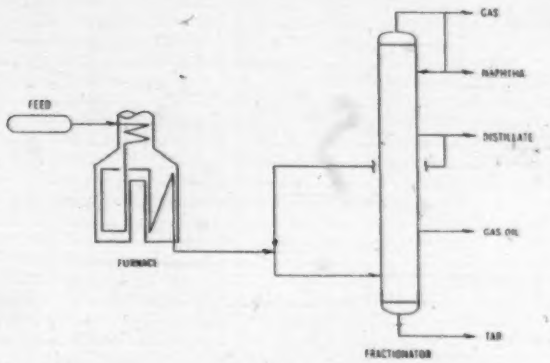

Figure 2.3: Coil Visbreaking Process [9]

drum temperature, and K_P= pressure correction factor at the mean drum pressure. The value of SVF ranges from 0.03 for the heavy residues to 1.2 for the light gasoils. But since the calculation of SVF requires pressure and temperature profiles along the reactor, exit product yields are also used in commercial units as the measure for visbreaking severity.

Yan [11] has used another method to define visbreaking severity at a reaction temperature T, in terms of the Equivalent Residence Time (ERT) at 427°C. The ERT is calculated as:

$$\text{ERT} = exp\left(-\frac{E_A}{R}\left(\frac{1}{T}-\frac{1}{700}\right)\right)t \tag{2.5}$$

where t= residence time, T= Reaction temperature in Kelvin, E_A= Activation Energy, and R= Gas constant. This definition of visbreaking severity has been used for this research and the ERT is referred to as the *Severity Index (SI)*.

The SI therefore depends upon the process conditions like the residence time and the reaction temperature and also the activation energy E_A. The activation energy E_A in turn, depends on the heavy oil and the reaction pathways concerned. Olmstead and Freund [12] have found that the activation energy for weight percent conversion of 698°C+ fraction during thermal cracking of the Arab heavy and Cold Lake residues to be almost the same at 212.8 and 215.5 kJ/mol, respectively. Yan [13] has found that

the activation energy of coke formation for visbreaking of the Arab heavy, Boscan and Mixed residues for 75/25 n-heptane and toluene coke (PA-coke) to be at 93 kJ/mol and that for n-heptane coke (P-coke) to be at 30.2 kJ/mol. Likewise, it can be assumed that the activation energy for different visbreaking reaction pathways yielding different products are almost similar for different feeds.

During visbreaking a part of the fluid experiences cracking at a much higher severity than the bulk of the fluid. In coil visbreaking, this is the boundary layer fluid in the furnace tubes where at the end of the furnace the temperatures are 30-40°C higher than the bulk fluid temperatures. In the soaker vessel due to back mixing, the fluids near the walls have a much higher residence time than the bulk fluid, which increase the visbreaking severity faced by this fluid [9]. This over-cracking of fluid near the walls leads to coke formation and deterioration in fuel stability at a much higher rate in these localized areas, even when the visbreaking severity experienced by the bulk liquid is much lower.

2.2.1 Coke Formation

The run length in a visbreaker is determined by the coke formation in the coils and the soaker vessel. The coke formation, which occurs on the heater tube walls and on the shell in the soaker vessel, is due to the high temperatures and longer residence time in fluid-flow zones with low turbulence, whereas the short residence time-low temperature conditions in a visbreaker help avoid coking in furnace tubes and soaker vessel. The petroleum residue is a mixture of the saturates, aromatics, resins and asphaltenes where the asphaltenes are peptized by the aromatics and resins. Coke formation occurs due to the separation of a hydrogen-lean and carbon-rich second liquid phase. This second phase is the precursor for coke formation. Experimentally, it has been observed that coke formation has an induction period and it is determined by the onset of this second liquid phase [14] [15]. It has been postulated that the peptizing agents, the aromatics and the resins, upon cracking lose their side chains and their peptizing power, whereas the asphaltenes also lose their side chains and alkyl groups and thereby become insoluble [13]. This second phase or the mesophase as it is called, shows up as bright parts among the dark amorphous coke and oil

part, when observed under cross-polarized light with an optical microscope [16]. The amorphous coke is formed after asphaltene has separated out from the oil and is then exposed to high temperature and does not show up bright under the cross-polarized light. The visbreaking coke really, is the onset point of coke formation during thermal cracking and the amount of coke increases with the increase in cracking severity. The maximum coke which is produced under severe thermal cracking conditions characterized by molecular rearrangements, dehydrogenation and polymerization reactions, has been found proportional to the Conradson Carbon Residue (CCR) of a feedstock. The CCR is determined under severe pyrolysis conditions [17].

2.2.2 Fuel Stability

The other constraint faced during visbreaking with increase of severity is its impact on the product stability. The maximum conversion in a visbreaker is limited by the storage stability of the final bottom product and this limits the visbreaking reaction severity. During thermal cracking, the aromaticity of the asphaltenes increases while that of the remaining oil or the maltenes decreases and this causes a reduction in the stability of the oil. As well olefins can be produced and polymerise to form gums. The product stability, which is the measure of asphaltene precipitating out of the product as sediment and then forming sludge or solids on storage or on filtration, is not only dependent upon the residue from the visbreaker unit but also on the cutter stocks used for further reduction of viscosity. Around the world, the fuel oil stability is measured using various test methods like the ASVAHL test method or the Merit number test, the ASTM D4740 or the spot test and the ASTM D4870 or the hot filtration test [5]. Among these, the hot filtration tests are the most widely used as they indicate accelerated, potential and total sediment value for the fuel oil (ASTM D4870, ASTM D4870 - Appendix A and ASTM D4870 - Appendix B). Apart from these, the Shell P value is also used to measure the product stability and the stability of fuel oil blends. If the P value is more than 1, the product is stable and the vice versa. In reality, a minimum P value of 1.2 is targeted when preparing fuel oil blends. The P value is defined as:

$$\text{P value} = \frac{P_0}{FR_{max}} \tag{2.6}$$

where P_0= peptizing power or the available aromaticity, and FR_{max}= Flocculation ratio or the aromaticity required to keep asphaltenes in solution.

Another method that has been used to measure the stability of asphaltenes in crude oils and also applies equally to the refinery streams is the Colloidal Instability Index (CII) [18]. This is the ratio of the asphaltenes and its flocculants (the saturates) to the sum of its peptizers (the aromatics and the resins).

$$CII = \frac{asphaltenes + saturates}{aromatics + resins} \tag{2.7}$$

On the basis of a large database of crude oil, it has been seen that if the CII<0.7, the solution is stable and if the CII>0.9, it is unstable. The values 0.7-0.9 lie in the uncertain zone.

2.3 Previous Work on Visbreaking Kinetic Models

Mild thermal cracking (visbreaking) and its kinetic modeling has been studied by many researchers. Visbreaker kinetic models over time, have moved from two lumped simplistic models to complex mechanistic models.

Singh et al. [19] studied the thermal cracking behavior of heavy feedstocks of Indian and Middle East origin between temperatures 400-430°C and evaluated the kinetic parameters of overall conversion of these feedstocks. The thermal cracking was found to follow a first order reaction kinetics and the activation energies for overall conversion were in the range of 102-206 kJ/mol. The difference in the activation energies of the feeds was attributed to the different saturate and asphaltene content in the feeds. Lower activation energy in one feed was attributed to the presence of more alkyl groups attached to the naphthenic and polar aromatic compounds. The product yields for gas, gasoline (IBP-150°C), light gasoil (BP: 150-350°C) and vacuum gasoil (BP: 350-500°C) was determined at different reaction temperatures and residence times. The product yields and their selectivity was explained with respect to the feed properties.

In an another thermal cracking study on Cold Lake bitumen, Shu and Venkatesan [20] used viscosity data to develop a kinetic model for visbreaking at conditions between 260-325°C and for residence time up to 720 hours. They found that visbreaking followed first order kinetics and calculated the activation energy (E_A) to be 130 kJ/mol and frequency factor (A_o) to be 8.18 x 10^9 hr^{-1}. The kinetic model used was a two-lump model with a feed pseudo-component cracking to a product pseudo-component.

Di Carlos and Janis [21] studied the visbreakability of atmospheric residues of Mediterranean and Italian origins at temperatures between 450-500°C and found that visbreaking followed first order kinetics. They estimated the kinetic parameters for overall conversion of the residue and concluded that paraffinic residues were more reactive than the residues rich in asphaltenes and resins at high temperatures and were more selective towards gasoil (BP: 175-370°C) due to the *splitting* reactions of the long chain alkanes, while residues rich in resins and asphaltenes show more selectivity towards gas and were more reactive at low temperatures due to the *dealkylation* reactions of the attached side chains.

In his work, Yan [11] conducted thermal reactivity experiments with one crude oil and two vacuum residues (BP: 550°C+) between reaction temperatures of 420-475°C with a coke yield up to 15wt%. The coke formation for all three feeds followed first order kinetics and it was found that the activation energy of coke formation for all three feeds was 93 kJ/mol. The coke yield was also found directly proportional to severity, which was defined as the equivalent residence time (ERT) in seconds at 427°C. The different feeds were characterized on the basis of their coking propensity, the ratio of the coke yield to the severity. The coking propensity of different residues was found to be related to the asphaltene content of the residue.

In a study on thermal cracking of the Aghajari long residue at temperature between 427-500°C and conversion (wt% of 150°C-) up to 15%, Krishna et al. [22] found the reaction kinetics to be of the first order and calculated the activation energy (E_A) and frequency factor (A_o) as 224.8 kJ/mol and 2.17 x 10^{12} s^{-1}. It was observed that gas, gasoline (IBP-150°C), kerosene (BP: 150-250°C) and gasoil (BP: 250-370°C) were produced whereas vacuum gasoil (BP: 370-500°C) and residue (BP:

500°C+) were depleted. A change in the cracking behavior was observed at a particular conversion level (7wt%). The gas and gasoline yield increase with severity was steady, however the kerosene yield increased sharply after 7 wt% conversion. Along with this, the increase in gasoil yield slowed down after 7 wt% conversion. This was explained because of the secondary cracking of gasoil to kerosene starting after this conversion level. The vacuum gasoil yield and the residue yield decrease also slowed down after 7 wt% conversion. It was hypothesized that most high molecular weight compounds got cracked and the cleavage of most alkyl substituents on condensed aromatic clusters occurred till conversion reached 7 wt%. After that, cracking reduced and the condensation or polymerization increased. This was corroborated by the steep increase in the conradson carbon residue content and the viscosity of 370°C+ fraction after a conversion level of 7 wt%.

Singh et al. [23] developed a four-lump kinetic model for the visbreaking of vacuum residues, asphalt and a refinery visbreaker feed from India at reaction temperatures 400-430°C. The model used three product lumps gas, gasoline (IBP-150°C) and light gasoil (BP: 150-350°C) and one feedstock lump (BP: 350°C+) with four reaction pathways to describe visbreaking. The kinetic parameters (rate constants and activation energies) were individually estimated for each reaction pathway using experimental data. The developed model could predict 75% of the data points with less than 15% error. The work concluded that while the feed cracked to gas, gasoline and light gasoil, the product light gasoil further cracked to make gasoline. The product residue portion was not considered as a lump and did not participate in the visbreaking reactions.

Singh et al. [24] also reported a five-lump and seven parameter model for the same feedstocks. The data prediction accuracy was within 20% for 70% of the data. Comparing this with the earlier four-lump model done on the same feedstocks but with different pseudo-component definition, it can be inferred that the activation energies depends upon the lump definition in a model. For instance, the activation energy for NGSR feed to gas fraction is 189.5 kJ/mol for the four-lump model whereas it is 194.7 kJ/mol for the five-lump model. Since the error analysis showed that the predictions of the two models has a similar percentage error, it can be concluded that

the increased complexity of the five-lump model serves no better than the four-lump model.

In another study, Kataria et al. [25] proposed a five-lump and a seven parameter model to explain the visbreaking of six different Indian heavy feedstocks. The kinetic parameters were different than the parameters evaluated by Singh et al. [24] even though for similar feedstocks and similar reaction pathways. This can lead to the inference that the kinetic parameters, in addition to the nature of feedstock and the degree of lumping, are also dependent on the mathematical method by which they are estimated. The product yields were correlated to the severity index (for E_A=50 kcal/mol) and feed properties. The activation energies of different reaction pathways were correlated to the feed properties using linear and power law models. The kinetic parameters depend on the variation of the structural parameters within the different lumps and upon the degree of lumping.

Castellanos et al. [26] developed a kinetic model, that has been used commercially for plant design and operation, with 51 pseudocomponents and 1225 reactions among them. The atmospheric and vacuum residue from Maya and Isthmus crude oils were characterized into different fractions on the basis of physical properties and these fractions were then divided into pseudocomponents based on carbon number. The model was based on first order kinetics and kinetic parameters were expressed as functions of molecular weights of the reacting and product compounds. The model parameters were calculated using plant data from an industrial Dubbs unit.

2.4 Carbon-types

Petroleum is a complex mixture of hydrocarbon molecules. The chemical and physical properties of a hydrocarbon molecule depend on how a carbon atom in the molecule is bonded to other carbon, hydrogen and hetero-atoms. Bonding or the sharing of electrons by the carbon atoms among themselves or with other elements determines the *type* of carbon. A complex hydrocarbon molecule has many different carbon-types. Examples of different carbon-types include aromatic, naphthenic, olefinic, paraffinic and branched paraffinic carbon. Thermal stability of petroleum hydrocarbons is dependent upon the bond dissociation energy (BDE) of the carbon-

carbon, carbon-hydrogen and carbon-sulfur bonds. The bond dissociation energy depends on the extent of overlap of the atomic orbitals of the nuclei and is affected by factors like resonance stabilization as in aromatic bonds and different types of bond strain. The C-C or C-H bonds formed by different carbon-types will have different bond dissociation energies and thus their stability and reactivity under thermal cracking conditions will differ. The carbon-carbon bond cleavage in benzene ring is not possible in mild thermal cracking due to the resonance structure which accords extra stability to the benzene ring (as compared to cyclohexatriene) [27]. Instead carbon-carbon cleavage is much more likely in the alkyl chains attached to the aromatics. The CH2 of an alkyl chain attached to an aromatic carbon in a polyaromatic hydrocarbon (PAH) molecule is less stable than that attached to an aromatic carbon of a monoaromatic ring.

Figure 2.4 shows the C-C bond dissociation energies calculated by Billaud et al. [28]. The β-bond is the weakest bond in the alkyl chain while the α bond is the most stable. All the other C-C bonds on the chain have similar energies.

bond	cleavage	bonding energy, kcal/mol
α	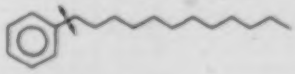	97.2
β		68.6
γ	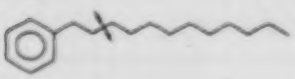	81.4
δ	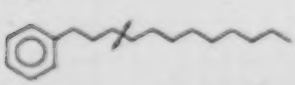	81.6
δ	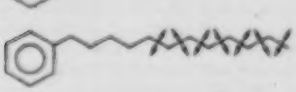	81.6

Figure 2.4: C-C Bond Dissociation Energy [28]

Similarly figure 2.5 presents the C-H bond dissociation energies as calculated by Billaud et al. [28]. This indicates that C-H bond cleavage is the most difficult at

the aromatic ring while it is the easiest for carbon at position 1 and therefore these hydrogen are referred to as *mobile*. The C-H bonds at other positions are equally strong and stronger than most C-C bonds on the alkyl chain.

hydrogen	cleavage	bond energy, kcal/mol
aromatic		110.9
aliphatic 1		81.7 (85)[a]
aliphatic 2	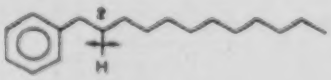	97.5 (≥95)[a]
aliphatic > 2	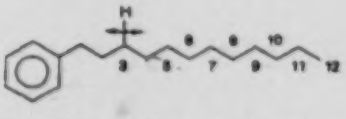	97.5

Figure 2.5: C-H Bond Dissociation Energy [28]

Figure 2.6 [29] shows the bond dissociation energies of the C-C and C-H bonds in 2-Dodecyl-9,10-dihydrophenanthrene (DDPh). The C-H bonds at the 9- and 10-positions with the BDE of 84.6 kcal/mol are the weakest bonds and thus the most likely places for hydrogen abstraction, followed by the benzylic hydrogen. The low BDE of 72.5 kcal/mol for the α C-C bond makes it an easy position for C-C bond cleavage during the β-scission reaction. Thus, it can be concluded that the bond dissociation energies help determine the most probable and favored reactions during thermal cracking.

V. Van Speybroeck et al. [30] have classified the polyaromatic hydrocarbons (PAHs) into six groups based on number of rings and have shown that the bond dissociation energy of the C-H bonds attached to the condensed ring aromatics are lower due to less stability of the molecule due to steric hindrance. This renders their free radicals more stability due to relief of steric hindrance.

Figure 2.7 shows the bond dissociation energies have been used to segregate aryl

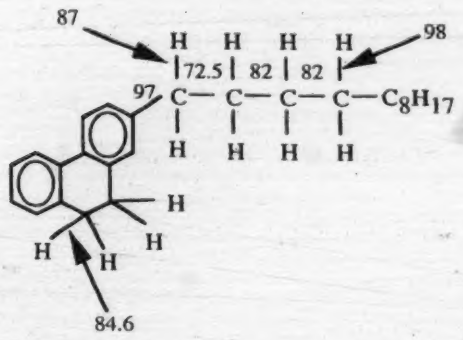

Figure 2.6: Bond Energies for 2-Dodecyl-9,10-dihydrophenanthrene [29]

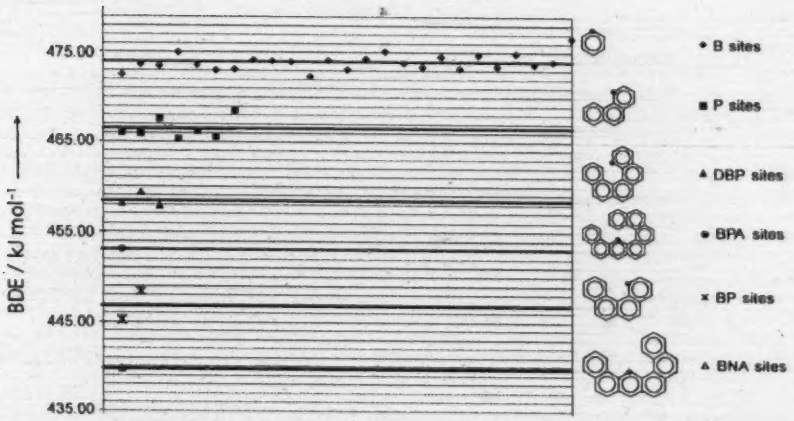

Figure 2.7: BDEs of Aryl Radicals of Six Different Groups of PAHs [30]

radicals into benzene like sites (B), phenanthrene like site (P), dibenzophenanthrene like site (DBP), benzophenanthreneanthracene like site (BPA), benzophenanthrene like site (BP) and benznaphtanthracene like site (BNA). The BNA radicals with the lowest BDE are the most stable among them.

2.4.1 Role of Nuclear Magnetic Resonance (NMR) Spectroscopy in Quantification of Carbon-types

NMR spectroscopy plays a prominent role in the structural analysis of petroleum fractions. Both proton (1H) and carbon (13C) NMR spectra can be used to quantify different carbon-types present in oil. Thus, the carbon-type content of the pseudo-components before and after cracking can be measured. As carbon-type actually means carbon *bond* type, the information reveals the net chemistry that has occurred during the process. Carbon-type analysis in this fashion quantifies the interconversion of one carbon-type into another during cracking. Depending upon the contents of particular carbon-types in a visbreaker feed, the *crackability* of the feed can also be predicted. In the present work, NMR structural analysis is performed on all pseudo-components before and after cracking. NMR data gives content information for over 80 types of different carbon species including aromatic, cycloparaffinic, branched paraffinic, paraffinic, and olefinic carbon. In addition, the NMR data reveals the average chain-length, the aromatic and naphthenic ring cluster sizes and the α-to-aromatic cycloparaffins present in the pseudo-components. Figure 2.8 details the different carbon-types that have been analyzed and quantified for the present research.

2.5 Thermal Cracking Mechanism

Thermal cracking occurs through a free radical chain reaction mechanism. The free radicals are formed upon bond breaking where one electron is shared by each fragment. Such type of bond breaking, which occurs during thermal cracking, is called homolysis and the energy involved is called homolytic bond dissociation energy. The hydrocarbon pyrolysis mechanisms proposed for thermal cracking of different classes of hydrocarbons are based on the free radical chain reaction mechanism

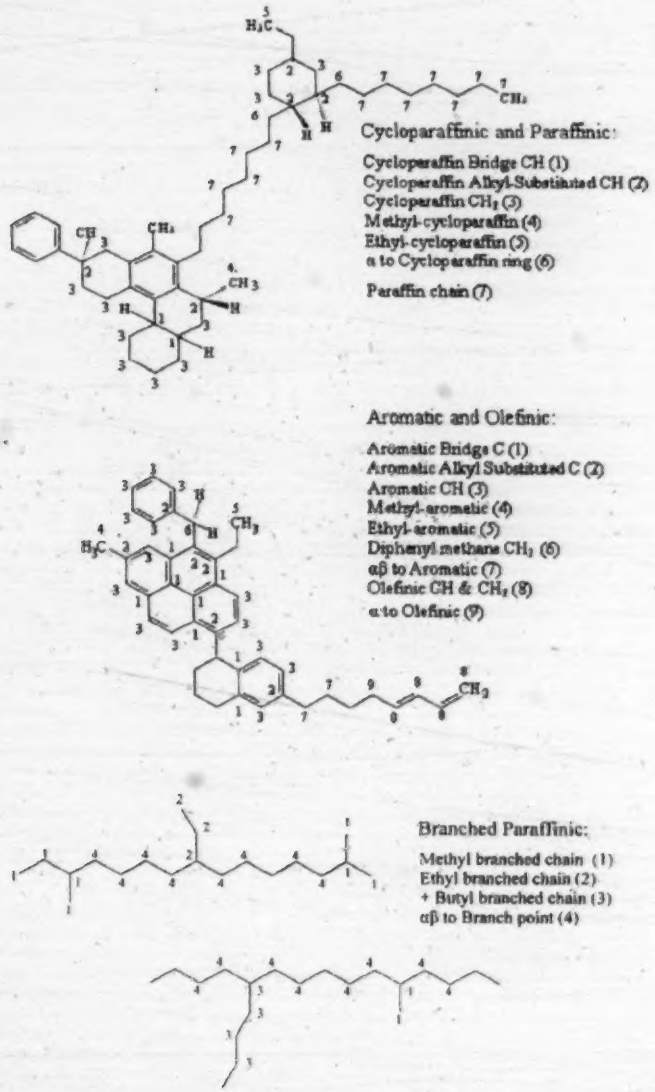

Figure 2.8: NMR Carbon-types

developed by Rice and Herzfeld [31] and Kossiakoff and Rice [32] for n-alkanes and further developed by the work of Fabuss, Smith and Satterfield [33][34]. Though the mechanism involves multiple reversible free radical reactions like homolytic dissociation, disproportionation, isomerization, β-scission and hydrogen abstraction [34], it is organized in three steps: initiation, propagation and termination, which are about net production, interconversion and net destruction of free radicals, respectively [35]. The activation energy of the three steps have been calculated by Billaud et al. [28] as:

Table 2.1: Activation Energy in kcal/mol

Steps	Reactions	Activation Energy
Initiation		80-85
Propagation	C-C bond cleavage	30
	hydrogen transfer	12-15
Termination		0

In the reaction mechanism, the initiation step has the highest activation energy (equal to the bond dissociation energy for homolytic cleavage) and once the radicals are formed, they go through a series of propagation reactions before termination since the activation energy for these steps are much lower. Gray and McCaffrey [36] showed that the high activation energy for the initiation step plays a much smaller role in determining the overall activation energy for cracking which is much lower because of the propagation and termination steps.

2.5.1 Initiation

The initiation step in thermal cracking is generally believed to take place though C-C bond cleavage as the bond dissociation energy of the C-C bond is lower than that of the C-H bond. However, in their study on liquid-phase and gas-phase thermal cracking of n-hexadecane, Wu et al. [37] have concluded that the initiation reaction also takes place through C-H bond cleavage resulting in production of H_2 gas in both liquid as well as gas phase cracking. Apart from the homolytic dissociation, another reaction responsible for the initiation step is bimolecular reverse radical disproportionation (RRD). An example of RRD is during the pyrolysis of methylpyrene

where hydrogen transfer from the benzylic carbon to an aromatic ring produces a methylpyrenyl radical and a methylhydropyrenyl radical [38] .

2.5.2 Propagation

The propagation step consists of multiple parallel sets of β-scission and hydrogen abstraction reaction. In a particular set, the hydrogen abstraction by a radical from a reactant molecule produces a reactant radical that undergoes C-C bond cleavage at the β position to the radical center to reproduce a radical and an olefin [34]. The most abundant product would come from a set where the weakest C-H bond is attacked for hydrogen abstraction and the weakest C-C bond is attacked for β-scission reaction [39]. The chain propagation is a radical conservation step. It has been shown by Wu et al. [37] that during liquid phase cracking, due to higher molecular density, the β-scission and hydrogen abstraction reactions have an equal probability whereas the gas phase cracking is more selective towards the β-scission reaction. The other reactions through which the propagation occurs are radical hydrogen transfer (RHT), where a hydrogen is transferred from a radical to an acceptor, addition reactions, where hydrogen and methyl radical are added to an acceptor and elimination reactions, where hydrogen and methyl radical are eliminated from a donor radical [38].

2.5.3 Termination

The chain termination steps take place through radical recombination and disproportionation reactions.

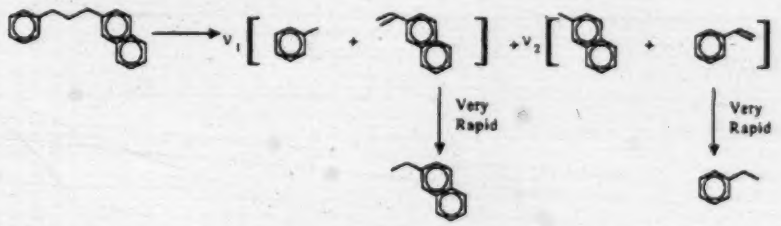

Figure 2.9: PPN Pyrolysis Pathways [40]

Figure 2.9 shows the reaction pathways or the reaction network responsible for

the production of the most abundant product pairs in the thermal pyrolysis of 2-(3-phenylpropyl)naphthalene (PPN) between 365-450°C and the residence time of 10-240 minutes and figure 2.10 shows the the different reactions that make the PPN pyrolysis reaction mechanism [40].

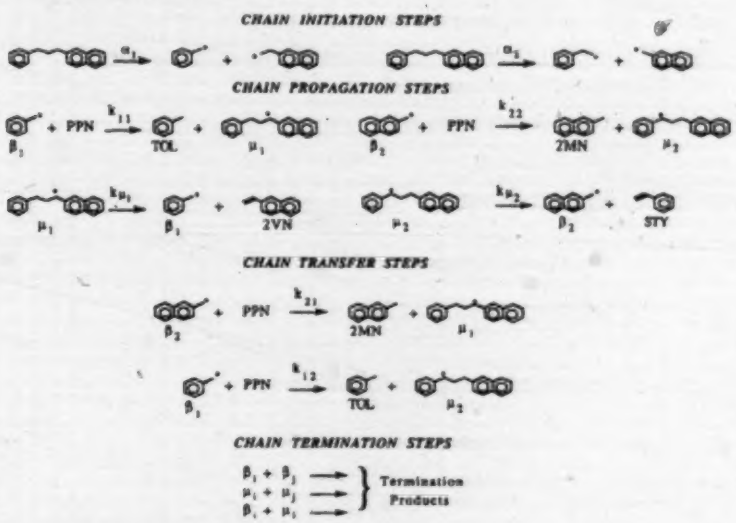

Figure 2.10: PPN Pyrolysis Mechanism [40]

2.5.4 Structure-Reactivity Relationships

The study of pyrolysis of heavy oils requires the prediction of the reactivity of different classes of hydrocarbons comprising these heavy oils during thermal cracking conditions. Researchers have for long studied the relationship of molecular structure with reactivity and have also put forth both empirical and mechanistic models for different hydrocarbon classes. Berman and Petrov [41], through calculation of relative rate constants of the cleavage of alkyl chains from condensed naphthenic hydrocarbons, concluded that the thermal stability of the cycloparaffins decreases as the number of rings and length of chains increases while the type of ring chain also has a bearing on the rate of cracking. Savage et al. [42] correlated the reaction rates of thermal cracking of polycyclic alkylaromatics with the Dewar reactivity numbers and showed that they affect the pyrolysis pathway adopted by the compound. The

structure reactivity relationships for one and two ring saturated cyclic compounds was reviewed by Savage et al. [43] and they proposed a new correlation for the reactivity of polycyclic perhydroarenes based on the characterization number (n). The characterization number is based on group additivity (12 for the cyclohexane ring, 4 of each CH2 group in the alkyl chain, 2 for the terminal methyl group in the chain and -1 for CH bond in the ring) and was proposed by Fabuss et al. [44]. Figure 2.11 presents the relationship of the rate constants with the characterization numbers.

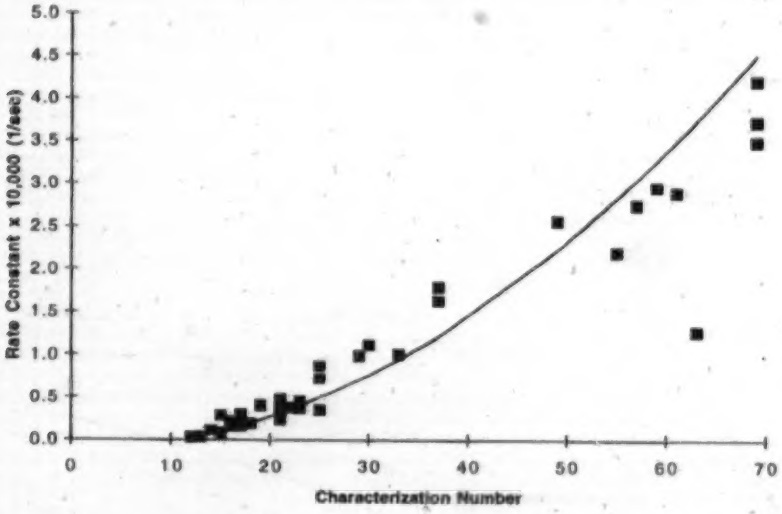

Figure 2.11: Empirical Structure-Reactivity Relationship for Saturated Cyclic Compounds [44]

Savage et al. [45] also proposed a mechanism based equation for structure reactivity relationship for alkylcyclohexane pyrolysis. This was based on the pyrolysis reaction mechanism and its kinetics. Figure 2.12 shows the experimental and the calculated first order rate constant for the conversion of n-alkylcyclohexane and shows its dependence on the alkyl chain length.

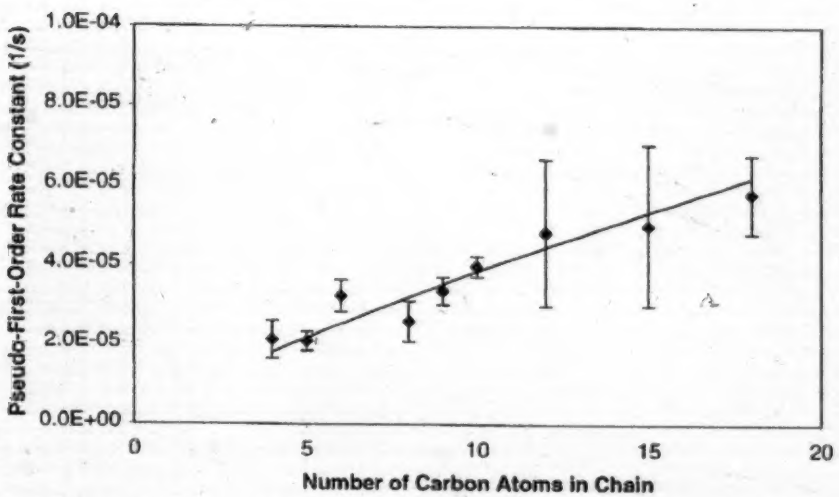

Figure 2.12: Mechanistic Structure-Reactivity Relationship for Saturated Cyclic Compounds [45]

Chapter 3

Experimental Work

This chapter describes the experimental work performed by the technical staff of the National Centre for Upgrading Technology (NCUT), Devon, Alberta. The present work is aimed at validating and extending the approach, previously used for developing a mathematical model for visbreaking of Athabasca bitumen, by applying the same approach to six different heavy oils representing feedstocks of different thermal reactivity from all around the globe. These six oils are Athabasca bitumen and Wolf Lake from Western Canada, Kern River from the USA, Kuwait from the Middle East, Rubiales from South America and Shengli from China.

3.1 Experimental Visbreaking Conditions

Thermal cracking of each feedstock was performed in a 1-liter continuous stirred-tank reactor (CSTR) autoclave where two runs were performed using 400 grams of feed. The reactor was flushed with nitrogen prior to heating and reached a maximum pressure of in the range of 300-500 psig at the temperature 405°C, depending on the gas-make. The run time was 30 minutes. The volume of gas was measured by a gas meter as the gas was transferred into a gas bag at the room temperature of 20°C. The contents of the gas products are the averages of the results for two runs under same conditions for each feedstock. The total liquid products for the two runs were combined and sent for analyses.

3.2 Fraction Preparation

The feed and total liquid product (TLP) were fractionated into naphtha (IBP-204°C), gasoil (204-524°C), and residue (524°C+) using the American Society for Testing and Materials [46](ASTM) D1160 method. The separation of these fractions into saturates, aromatics, resins or polars and asphaltenes (SARA) was done using the following procedure. Asphaltenes were precipitated from the D1160 vacuum residue (524°C+) with pentane, using a single treatment of the procedure outlined in Peramanu et al. [47]. The gasoil and the residue maltenes were separated into saturates, aromatics and polar fractions using a modification of the clay-gel adsorption chromatography method described in Peramanu et al. [47].

3.3 Characterization of Pseudo-components

3.3.1 Gas Analysis

The gas analysis was run on the gas product on a Refinery Gas Analyzer (MTI).

3.3.2 Elemental Analysis

Sulfur contents of naphtha were measured using x-ray fluorescence (ASTM D4294) on a Horiba XR Fluorometer (SLFA-1800). The sulfur content of the gasoil saturates were measured by GC (HP 6890) using sulfur chemiluminescence detection (ASTM D5623). The sulfur contents of all other samples were measured using a Leco SC 432 analyzer where ASTM D1552 was used for the aromatics and polars and ASTM D4239 was used for asphaltenes. The nitrogen contents of the naphtha and saturates were measured using the ASTM D4629 method on a Dohrman Nitrogen Analyzer (DN-1000). The carbon and hydrogen content of saturates was measured using the ASTM D5291 method on a Perkin Elmer 2400 analyzer. The carbon, hydrogen, and nitrogen contents of the aromatics, polars and asphaltenes were measured on a Leco 1000 Analyzer using ASTM D5291 for the aromatics as well as polars and ASTM D5373 for the asphaltenes. The carbon and hydrogen content of the naphtha were measured on the Leco 1000 Analyzer using the ASTM D5291 procedure.

3.3.3 Coke Content

Conradson carbon content of the feed and TLP was measured using the microcarbon residue (MCR) test procedure (ASTM D4530). The toluene insolubles contents were obtained by soxhlet extraction of the feed or TLP residue (524°C+) using ASTM D4072.

3.3.4 Nuclear Magnetic Resonance Spectroscopy

1H NMR samples were prepared by mixing approximately 20 mg of the sample with 700μL deuterochloroform (CDCl3). For 13C NMR spectra, approximately 50 mg of asphaltenes and 100 mg of all other fractions were used in either 700μL or 600 μL CDCl3, respectively. The NMR experiments were performed at room temperature (20 $\pm$ 1°C) on a Varian XL-300 NMR spectrometer, operating at 299.943 MHz for proton and 75.429 MHz for carbon. The proton spectra were collected with an acquisition time of 2.1 s, a sweepwidth of 7000 Hz, a pulse flip angle of 30.8° (8.2 μs), and a 1-s recycle delay. These pulse recycle conditions permit the collection of quantitative spectra for all protonated molecular species in the petroleum samples where the maximum spin lattice relaxation time (T1) is expected to be less than 20 s. The spectra, resulting from 128 scans and using 0.33 Hz line broadening, were referenced to the residual chloroform resonance at 7.24 ppm. The quantitative carbon spectra were acquired using an acquisition time of 0.9 s and a sweepwidth of 16,500 Hz. For naphtha and gas oil samples, a flip angle of 26.2° (4.6μs) and recycle delay of 10 s were used, and for the residue samples, a flip angle of 31.9° (5.7μs) and a 4-s delay were used. These parameters are quantitative for carbons with spin lattice relaxation times (T1) of the order of 100 s in distillate and 30 s in the residue. Reverse-gated waltz proton decoupling was used to avoid nuclear Overhauser effect enhancements of the carbon signals. The spectra were the result of 5000 scans for the naptha and gas oil fractions (524°C-) and 15,000 scans for the residue fractions (524°C+). Line broadening was used to improve the signal-to-noise ratio of the spectra. Naphtha and saturates spectra used 5 Hz, aromatics and polars spectra used 10 Hz, and asphaltenes spectra used 15 Hz line broadening. All spectra were referenced to the CDCl3 resonance at 77.0 ppm. Carbon-type analyses were

performed using proton and carbon NMR spectra and elemental analysis results, using a procedure based on that described by Japanwala et al. [48].

Chapter 4

Model Data and Approach

4.1 Model Data

The first half of this chapter presents the results of the extensive lab analysis conducted on different feed and visbroken product samples. The nuclear magnetic resonance (NMR) carbon-type analysis, which is the quantification of carbon-types in the feed and the visbroken product, is the heart of this extensive lab work performed at the National Centre for Upgrading Technology (NCUT), Devon, Alberta. The second half of the chapter introduces the approach adopted for developing this model using NMR carbon-type analysis. It includes a discussion on the lab results and the pyrolysis behavior of the model compounds that resemble molecules or molecular units in the heavy oils chosen. The pyrolysis studies of these representative model compounds help us determine the main reactions behind visbreaking.

4.1.1 Pseudo-component Content in Feed and Product

Figure 4.1 shows the mass of different pseudo-components obtained after the distillation and SARA analysis of feed and product.

4.1.2 Gas Component Analysis

Figure 4.2 shows the components of gas obtained after visbreaking of different oils. A complete list of gas components after chromatographic analysis is listed in Appendix A.

Mass balance: Basis 100 gms of feed												
	Athabasca		Kuwait		Rubiales		Shengli		Wolf Lake		Kern River	
	Feed	Product	Feed	Product	Feed	Product	Feed	Product	Feed	Product	Feed	Product
Gas		2.6		0.79		0.6		1.3		2.0		1.0
Naphtha (IBP-204°C)	0.6	7.7	9.7	14.5	1.7	3.5	6.2	8.0	2.7	5.4	0.9	5.1
Gas oil (204-524°C)												
Saturates	18.5	22.6	24.2	26.4	36.6	36.2	36.9	36.8	19.4	23.4	26.6	28.2
Aromatics	23.9	30.3	23.6	27.8	26.2	24.6	14.5	17.2	24.2	29.7	27.8	30.6
Resins	2.4	3.1	1.3	1.8	2.6	2.4	1.7	2.3	1.5	2.9	5.1	6.7
Sub-total	44.8	56.0	49.1	56.1	65.4	63.2	53.0	56.3	45.1	56.0	59.5	65.6
Residue (524°C+)												
Saturates	2.2	1.2	3.2	1.8	3.1	3.1	6.1	6.2	2.9	1.8	2.3	1.4
Aromatics	19.2	11.2	18.6	10.3	8.6	8.9	14.7	11.9	22.1	12.1	13.3	8.4
Resins	13.5	4.7	9.8	5.3	3.7	3.5	13.2	9.0	10.2	7.5	16.5	10.1
Asphaltenes	19.8	16.6	9.6	11.2	17.6	17.2	6.9	7.4	17.0	15.2	7.5	8.4
Sub-total	54.6	33.7	41.1	28.6	32.9	32.6	40.8	34.5	52.2	36.6	39.6	28.3
Total	100.0	100.0	100.0	100.0	100.0	100.0	100.0	100.0	100.0	100.0	100.0	100.0

Figure 4.1: Pseudo-component Content in Feed and Product

Mole Percentage						
Component	Athabasca	Kuwait	Rubiales	Shengli	Kern River	Wolf Lake
H_2S	21.4	8.7	9.7	3.0	6.6	18.7
$CO+CO_2$	5.9	3.7	5.9	4.0	10.9	3.3
H_2	6.4	8.6	9.1	10.4	5.7	8.5
C_1	36.0	57.1	51.2	61.2	54.2	43.9
C_2	14.8	13.0	13.9	11.1	12.4	13.5
C_3	9.5	4.9	7.0	5.4	6.8	7.3
C_4	3.9	2.2	2.1	2.5	2.0	2.8
C_5+	2.1	1.7	1.2	2.4	1.4	1.9
Total	100.0	100.0	100.0	100.0	100.0	100.0

Figure 4.2: Gas Component Analysis

Athabasca Bitumen					
Elemental - Feed					
Fraction	Carbon	Hydrogen	Nitrogen	Sulphur	Total
Feedstock	84.8	10.0	0.4	4.8	100.0
Naphtha	87.1	11.5	0.3	1.1	100.0
Gas oil	85.1	11.5	0.2	3.3	100.0
GO-S	86.4	13.6	0.0	0.0	100.0
GO-Ar	84.0	10.1	0.2	5.7	100.0
GO-R	86.0	8.7	0.9	4.4	100.0
Resid	84.8	8.3	0.5	6.3	100.0
R-S	86.6	13.3	0.0	0.1	100.0
R-Ar	84.7	10.2	0.2	5.0	100.0
R-R	85.1	8.4	0.6	5.9	100.0
As	83.4	7.6	0.8	8.2	100.0
Elemental - TLP					
Feedstock	85.0	9.9	0.5	4.6	100.0
Naphtha	84.6	13.4	0.0	2.1	100.0
Gas oil	85.2	11.0	0.2	3.5	100.0
GO-S	86.1	13.8	0.0	0.1	100.0
GO-Ar	85.3	9.7	0.1	5.0	100.0
GO-R	85.7	8.0	1.4	4.9	100.0
Resid	85.4	7.6	0.8	6.2	100.0
R-S	85.8	14.0	0.0	0.1	100.0
R-Ar	86.2	9.3	0.2	4.4	100.0
R-R	86.0	8.6	1.0	4.4	100.0
As	85.2	5.9	1.3	7.6	100.0
Subtotal	85.2	10.0	0.4	4.3	100.0

Figure 4.3: Elemental Analysis

4.1.3 Elemental Analysis

Figure 4.3 shows the carbon, hydrogen, nitrogen and sulfur elemental analysis for Athabasca bitumen feed and its visbroken product. Similar analyses were conducted for all different oils and their visbroken product. It is to be noted that the hydrogen content of resins and asphaltenes are the lowest among all pseudo-components.

4.1.4 Coke Yield

Figure 4.4 shows the microcarbon residue of the feed and the toluene insolubles of the total liquid product after visbreaking. The mass of toluene insolubles represent the coke formed during the visbreaking reaction and is different from the microcarbon residue which represents the maximum coke formed during severe pyrolysis (coking) of the feed.

	Weight Percentage	
	Micro-Carbon residue	Toluene Insolubles
Kern River	7.82	0.03
Shengli	5.70	0.11
Wolf Lake	12.50	0.25
Kuwait	8.60	0.50
Athabasca	13.10	1.59
Rubiales	11.90	3.37

Figure 4.4: Coke Yield

4.1.5 NMR Carbon-type Analysis

Figure 4.5 shows the carbon-types in mole percentage obtained from NMR spectroscopy and their derived parameters, like the aromatic and naphthenic cluster sizes and the average chain length, for Athabasca bitumen. This carbon-type analysis is performed for all pseudo-components in feed and total liquid product for all the oils studied. The carbon-type analysis report shows forty different carbon-types, in which there are four aromatic types, four naphthenic types, methyl and ethyl groups attached to the rings, chain attachments, branched paraffins, olefins and paraffin chain carbon-types.

4.2 Model Approach

4.2.1 NMR Carbon-type Analysis

In the present work, NMR structural analysis was performed on all pseudo-components before and after cracking. NMR data gives content information for over 80 types of different carbon species including aromatic, cycloparaffinic, branched paraffinic, paraffinic, and olefinic carbon. In addition, the NMR data reveals the average chain-length, the aromatic and naphthenic ring cluster sizes and the α-to-aromatic cycloparaffins present in the pseudo-components. From the perspective of residue conversion to distillates, the most relevant data is that of the residue fraction and its pseudo-components. The chemical nature of different oils under study is illustrated by different parameters in Figure 4.6. The most aliphatic feed among the oils is Shengli, whereas Athabasca bitumen is the most aromatic. Also Athabasca is

Sample:	AFN	AFGOS	AFGOAr	AFGOP	AFRS	AFRAr	AFRP	AFRAs	N	GO	R	Feed
Aromatic carbon (Mole % C)	8.28	2.18	43.58	41.51	4.91	45.52	42.64	46.51	8.28	26.36	43.56	35.64
α to aromatic cycloparaffin	0.00	0.00	2.03	1.25	0.00	1.06	1.49	1.57	0.00	1.15	1.31	1.23
Ar carbon cluster size	8.00	7.00	16.00	16.00	7.00	21.00	20.00	20.00	8.00	10.00	19.00	15.00
Cy carbon cluster size	10.00	8.00	7.00	8.00	7.00	7.00	8.00	12.00	10.00	8.00	8.00	8.00
Chain ends (Mole % C)	13.28	14.76	9.71	10.36	9.13	6.39	9.18	9.84	13.28	11.83	8.44	9.99
Chain midsection (Mole % C)	0.20	1.44	1.14	2.19	11.86	5.55	6.63	5.62	0.20	1.32	6.09	3.92
Average chain length	2.33	2.78	3.02	3.28	6.29	5.20	4.38	3.83	2.33	2.93	4.55	3.81
Chain Ends (Fraction)												
Ar	0.07	0.00	0.19	0.21	0.19	0.29	0.20	0.20	0.07	0.11	0.23	0.18
O	0.03	0.03	0.04	0.07	0.04	0.08	0.05	0.06	0.03	0.04	0.06	0.05
Cy	0.80	0.56	0.32	0.44	0.20	0.10	0.38	0.45	0.80	0.43	0.30	0.36
Br	0.02	0.14	0.12	0.02	0.25	0.11	0.05	0.03	0.02	0.12	0.07	0.10
P	0.09	0.26	0.12	0.14	0.31	0.25	0.15	0.10	0.09	0.18	0.18	0.18
S	0.00	0.00	0.21	0.12	0.00	0.17	0.16	0.16	0.00	0.12	0.16	0.14
Total	1.00	1.00	1.00	1.00	1.00	1.00	1.00	1.00	1.00	1.00	1.00	1.00
Carbon Type (mole%)												
Aromatic	8.28	2.18	43.58	41.51	4.91	45.52	42.64	46.51	8.28	26.36	43.56	35.64
Cycloparaffinic	60.99	53.38	21.38	26.62	43.29	22.27	24.09	25.05	60.99	34.88	24.57	29.41
Branched Paraffin	4.01	13.47	7.46	2.90	14.80	5.83	3.75	1.74	4.01	9.70	4.19	6.66
Paraffin Chain (>C2)	2.62	9.72	4.95	6.47	20.19	10.13	10.54	8.31	2.62	7.00	9.98	8.60
Olefin	0.45	0.53	0.45	0.73	0.49	0.62	0.51	0.64	0.45	0.50	0.59	0.55
Ring M & E & DPM	10.60	9.21	11.65	10.49	7.21	8.49	8.34	6.62	10.60	10.58	7.73	9.02
Chain attachments (a,b)	13.04	11.52	10.53	11.28	9.10	7.14	10.13	11.13	13.04	10.98	9.40	10.13
C=O*	0.00	0.00	0.00	0.00	0.00	0.00	0.00	0.00	0.00	0.00	0.00	0.00
Total	100.00	100.00	100.00	100.00	100.00	100.00	100.00	100.00	100.00	100.00	100.01	100.01
* C=O was not measured												
Carbon Type												
C=O*	0.00	0.00	0.00	0.00	0.00	0.00	0.00	0.00	0.00	0.00	0.00	0.00
Aromatic and Olefin												
Aromatic NS (C+CH)	1.59	0.04	3.47	4.43	0.10	3.63	4.91	7.54	1.59	2.10	5.22	3.80
Aromatic Bridge C	0.00	0.00	12.42	10.57	0.00	17.90	14.53	14.65	0.00	7.19	15.18	11.51
Aromatic Alkyl Subst. C	4.06	1.12	13.69	12.68	2.78	8.24	9.46	10.18	4.06	8.44	9.03	8.74
Aromatic CH	2.63	1.02	14.00	13.84	2.02	15.76	13.74	14.14	2.63	8.62	14.12	11.59
Methyl-Aromatic	1.86	0.32	2.99	2.93	0.26	1.26	1.35	1.75	1.86	1.89	1.42	1.63
Ethyl-Aromatic	2.48	1.02	1.81	2.10	1.13	1.10	1.03	1.45	2.48	1.50	1.21	1.35
Propyl-Aromatic	0.21	0.72	0.83	0.78	0.58	0.64	0.58	0.60	0.21	0.78	0.61	0.69
Diphenyl Methane CH2	0.00	0.00	1.80	1.86	0.00	1.11	1.27	1.22	0.00	1.06	1.15	1.10
Olefin CH	0.38	0.43	0.38	0.67	0.38	0.52	0.42	0.55	0.38	0.42	0.50	0.46
Olefin CH2	0.07	0.06	0.03	0.01	0.05	0.02	0.02	0.01	0.07	0.04	0.01	0.03
Olefin CH2(=C)	0.00	0.04	0.05	0.05	0.06	0.08	0.07	0.08	0.00	0.04	0.08	0.06
Cycloparaffin and Paraffin												
Cycloparaffin Bridge CH	11.31	4.16	1.55	3.48	0.93	0.31	3.05	6.12	11.31	2.73	3.12	2.99
Cycloparaffin Alkyl Subst. CH	15.30	14.18	6.86	6.88	6.42	4.68	6.99	5.61	15.30	9.89	5.66	7.61
Cycloparaffin CH2	34.38	35.00	12.92	16.20	35.89	17.19	13.98	13.24	34.38	22.22	15.71	18.74
Cycloparaffin C(=CH2)	0.00	0.04	0.05	0.05	0.06	0.08	0.07	0.08	0.00	0.04	0.08	0.06
Methyl-Cycloparaffin	3.05	3.86	2.49	0.99	3.31	3.10	2.34	0.08	3.05	2.98	1.83	2.35
Ethyl-Cycloparaffin	3.21	4.00	2.56	2.61	2.51	1.92	2.35	2.12	3.21	3.16	2.12	2.59
Paraffin Chain	2.41	8.99	4.11	5.69	19.61	9.49	9.96	7.71	2.41	6.21	9.37	7.91
Branched Paraffin												
Methyl-Branched Chain	3.68	12.78	6.63	2.81	14.25	5.83	3.75	1.74	3.68	8.97	4.17	6.31
Ethyl-Branched Chain	0.32	0.69	0.20	0.08	0.47	0.00	0.00	0.00	0.32	0.39	0.02	0.19
+Butyl-Branched Chain	0.02	0.00	0.63	0.00	0.08	0.00	0.00	0.00	0.02	0.34	0.00	0.15
Chain Attachments												
a to Sulphides	0.00	0.00	2.03	1.25	0.00	1.06	1.49	1.57	0.00	1.15	1.31	1.23
ab to Aromatic Rings	1.79	0.09	3.70	4.40	3.53	3.73	3.76	3.86	1.79	2.24	3.78	3.08
a to Olefin	0.38	0.43	0.38	0.67	0.38	0.52	0.42	0.55	0.38	0.42	0.50	0.46
a to Cycloparaffin Rings	10.64	8.32	3.09	4.59	1.85	0.62	3.47	4.47	10.64	5.33	2.77	3.96
ab to Branch Points	0.23	2.68	1.33	0.36	3.34	1.20	0.99	0.68	0.23	1.84	1.05	1.39
Total	100.00	100.00	100.00	100.00	100.00	100.00	100.00	100.00	100.00	100.00	100.01	100.01

Figure 4.5: NMR Carbon-type Analysis for Athabasca Bitumen

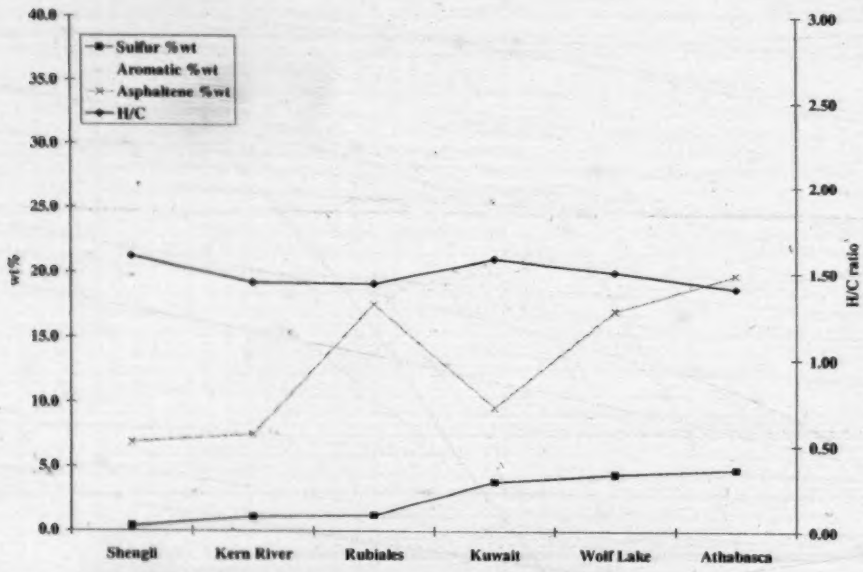

Figure 4.6: Chemical Nature of Different Oils

the most sulfur bearing oil, while Shengli is the least. It can also be seen that the hydrogen to carbon ratio and the asphaltene content are not a good indicator of the aromatic nature of the feed.

A comparison of the NMR carbon-type information of the residue fraction of different feeds reveals that the average aromatic cluster size varies from 13 carbons (2 to 3 rings) to 20 carbons (4 to 5 rings), where the largest clusters are present in Rubiales. The average cycloparaffinic ring cluster size for the residue varies from 7 carbons (1 to 2 rings) to 11 carbons (2 to 3 rings), with the largest clusters being present in Kern River. A comparison of the chain segment lengths in the residue fractions shows that the average length varies from 3.8 to 7.5 carbons, where the longest chain segments are in Shengli and the shortest in Rubiales. Different groups are attached to the chain segments that affect the reactivity of these paraffin chain segments in these feed molecules. Figure 4.7 shows the fraction of different carbon-types that are attached to the paraffin chain ends.

Figure 4.8 shows that after visbreaking, the aromatic cluster size in residue frac-

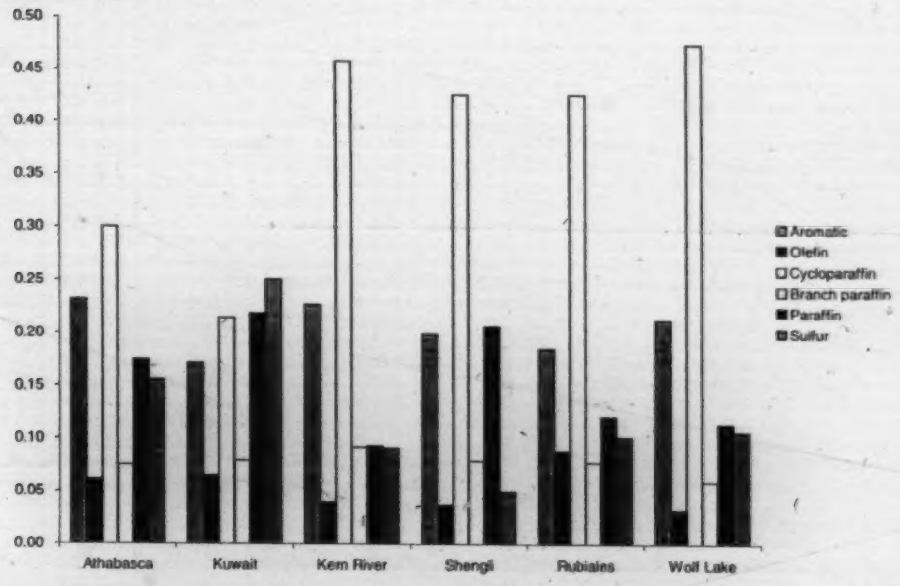

Figure 4.7: Fraction of Chain Ends in Residue

tion increases, whereas the chain length decreases.

Apart from the information on the relative amount of the carbon-types present in residue fraction of the feed, the NMR data indicates the degree of participation of different carbon-types in thermal cracking reactions from the net change of these carbon-types before and after cracking. To help understand the potential contribution of different carbon-types to the reactivity of the different oils, pyrolysis studies of model compounds under visbreaking conditions were reviewed.

4.2.2 Residue Conversion

Residue conversion is defined as the percentage change in the mass of residue fraction (524°C+) after visbreaking. Figure 4.1 shows that the more the residue is depleted, the more the gasoil content is increased after visbreaking. The percentage residue conversion in a visbreaker has been related to the asphaltene content, the saturate content and the aromaticity of the feed [9]. In the present study, at the same process severity, the residue conversion in Athabasca Bitumen is the highest followed

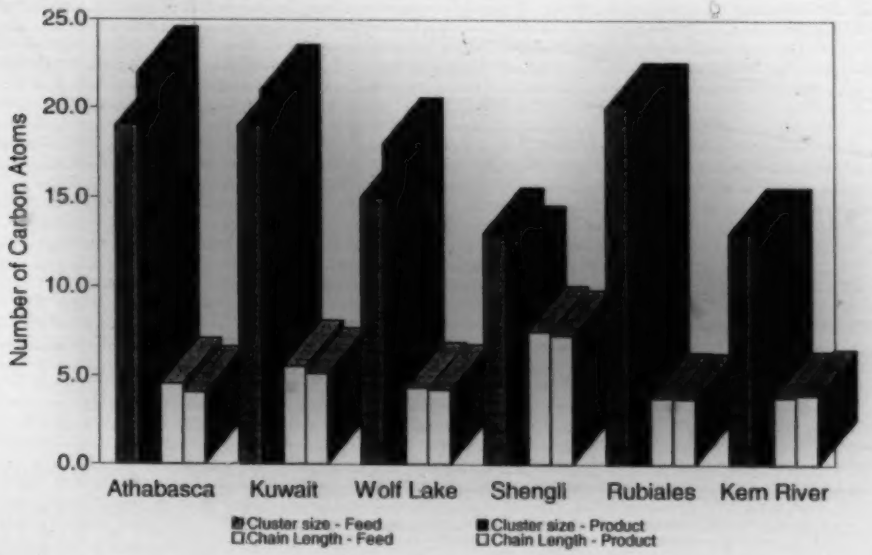

Figure 4.8: Change in Residue after Visbreaking

by Kuwait, Wolf Lake, Kern River and Shengli, while Rubiales practically did not convert. As shown in Figure 4.9, residue conversion does not correlate with the asphaltene content of the feed. In Figure 4.10, residue conversion seems to linearly correlate with the aromatic carbon content in the feed, but offers no explanation to almost nil conversion of Rubiales which has a significant 30.4 percent aromatic carbon content.

An important observation from the data is that at similar reaction severity, the percentage conversion of the respective pseudo-components varies from feed to feed as shown in Figure 4.11. For instance, the percentage conversion of residue saturates varies from 43.9 in Athabasca to -2.0 in Shengli. The difference in percentage conversion is even more pronounced in residue polars with 65.4 in Athabasca to 5.4 in Rubiales. In case of asphaltenes, while they convert to other pseudo-components in Athabasca and Wolf Lake and their quantity in the visbroken product reduces, there is a net addition to asphaltenes in Kuwait, Shengli and Kern River. These data help reinforce the understanding that these pseudo-components are not a homogenous chemical entity and their chemical composition and the reactivity under visbreak-

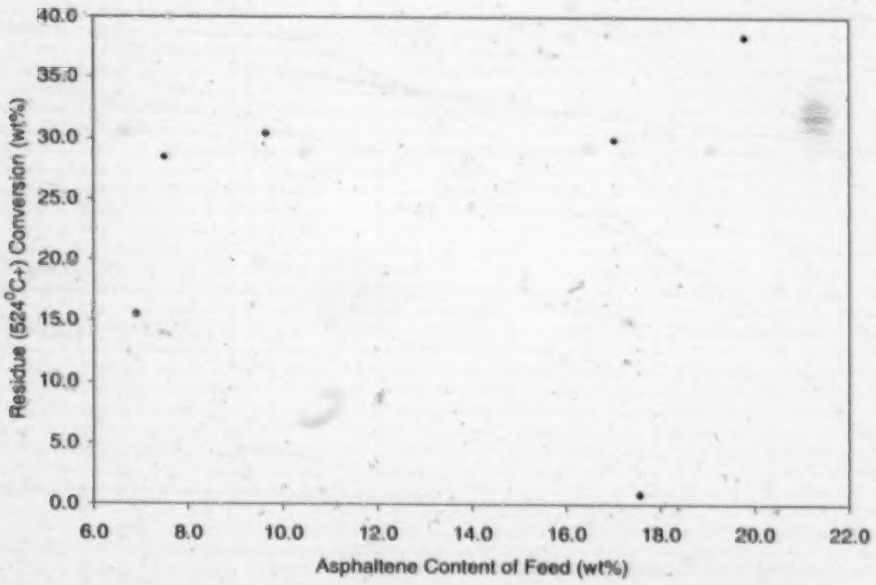

Figure 4.9: Residue Conversion vs. Asphaltene Content of Feed

ing conditions vary from feed to feed. Therefore, the reactivity of a visbreaker feed cannot be attributed to the individual composition of these pseudo-components viz. percentage of asphaltenes, aromatics or polars present. This complex behavior by petroleum fractions underscores the importance of the study of carbon-types and molecular structure in determining the reactivity of a feed.

4.2.3 Coke Formation and Carbon-types

Conradson carbon content, otherwise known as the microcarbon residue (MCR) content, is the most useful indicator of the coke formation tendency of an oil during a severe thermal cracking process like coking. The MCR of various asphaltenes has been found to be dependent on their NMR-derived aromatic carbon content as in Figure 4.12 [17].

While MCR is a good indicator of coke formation during coking, the coke formation during visbreaking does not correlate with the MCR content of the feed as in Figure 4.13.

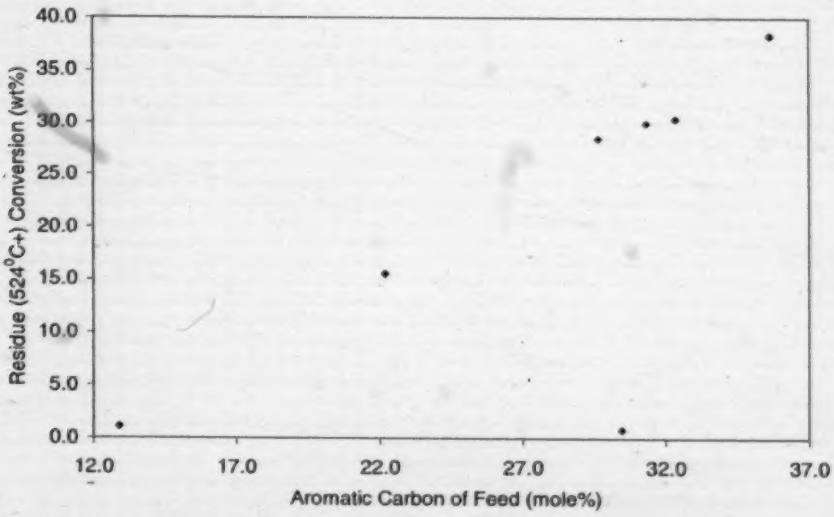

Figure 4.10: Residue Conversion vs. Aromatic Content of Feed

Coke formation during visbreaking is measured by the toluene insolubles content of the visbreaking product. Comparing the toluene insolubles of different feeds after visbreaking provides an insight into their coking tendencies at the onset of coking. For the present study the maximum coke formation under visbreaking conditions was observed in Rubiales, which shows almost no residue conversion. It has been suggested in the literature that at a single process severity, coke formation during visbreaking depends upon the asphaltene content of the feed [11]. However, for the present study the feed asphaltene content does not correlate with the toluene insolubles after visbreaking as shown in Figure 4.14.

4.2.4 Representative Model Compounds

The NMR carbon-type data from the residue and gasoil pseudo-components gives quantitative information about the ring sizes and the alkyl chain lengths and thus help in the selection of the representative model compounds. The average chain length in the asphaltenes ranges from 3.3 to 6.1 and is shorter than that of the residue aromatics which is from 3.9 to 7.9. The maximum chain length of 8.5 is in the residue saturates fraction in Shengli, which is an aliphatic feed. The maximum

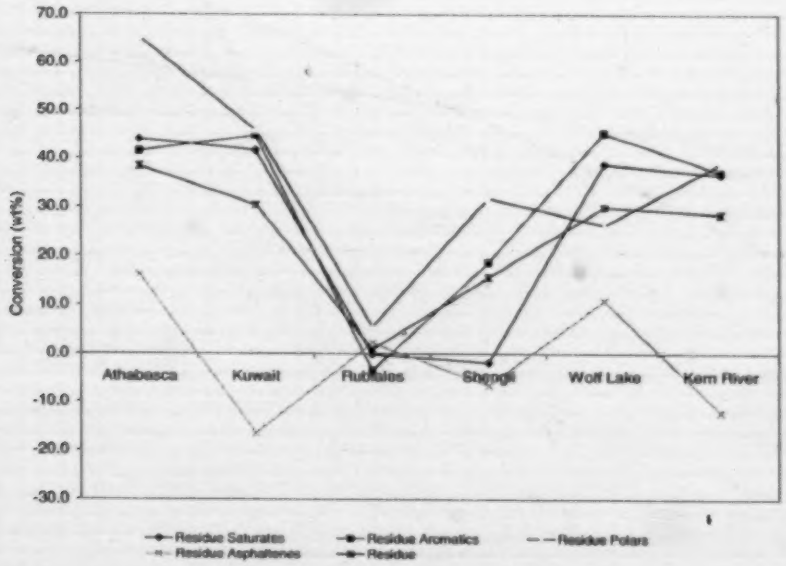

Figure 4.11: Percentage Conversion of Different Residue Pseudo-components

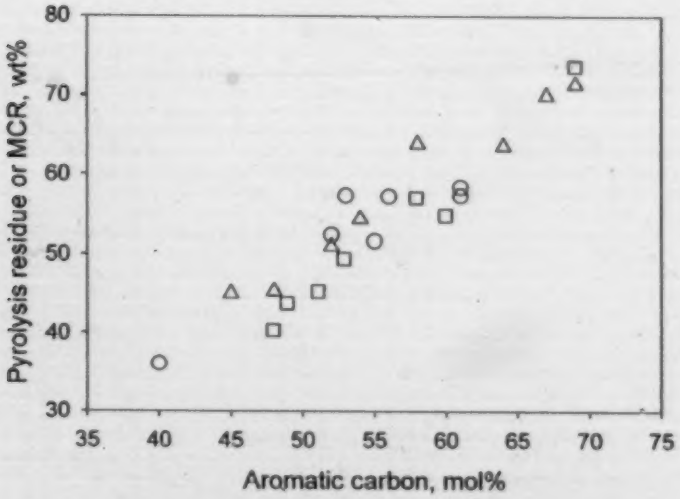

Figure 4.12: MCR vs. Aromatic Carbon Content [17]

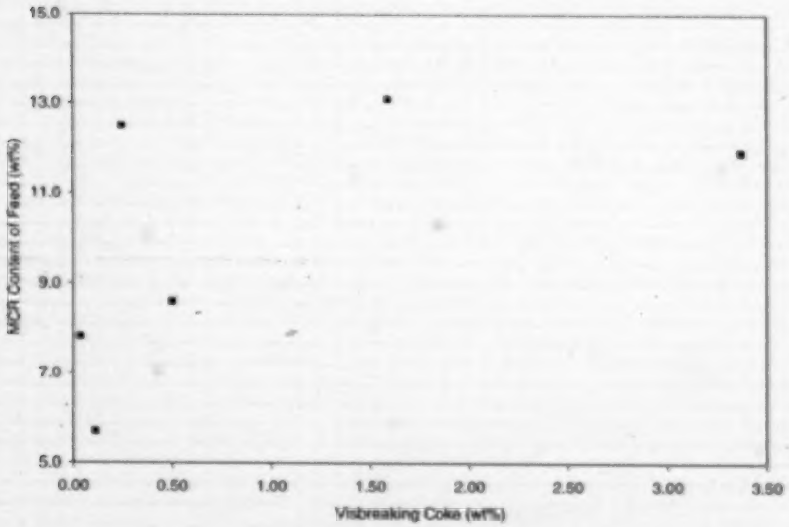

Figure 4.13: Visbreaking Coke vs. Feed MCR

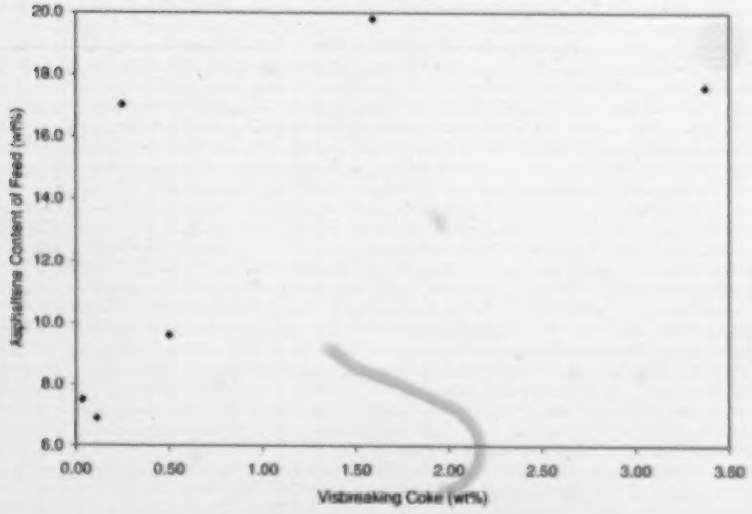

Figure 4.14: Visbreaking Coke vs. Feed Asphaltene

aromatic cluster size of 22 is in the asphaltene fraction of Rubiales. The aromatic carbon cluster size in the residue aromatic fraction range from 13 to 21. The maximum cycloparaffin carbon cluster size of 18 is in the gasoil aromatic fraction in Rubiales. The α-to-aromatic cycloparaffin species, whose behavior during visbreaking should be identical to the hydroaromatic model compounds, is the maximum in the gasoil polar and aromatic fractions. The complexity of chemistry in these pseudo-components makes simplified generalization about their pyrolysis behavior misleading. The knowledge of the kinetic data, reaction products and pathways of pyrolysis of the representative model compounds provides insight into the chemical behavior of identical moieties present in the visbreaker feeds. The literature provides many examples of pyrolysis of model compounds conducted at similar reaction severity. Four classes of model compounds that are relevant to visbreaking reactions at the experimental severity are listed in Figure 4.15 [1] [29] [49] [40] [43] [50] [51]. These classes are polycyclic alkylaromatics, polycyclic alkylcycloparaffins, 1,3-diarylalkanes and hydroaromatics.

Polycyclic Alkylaromatics

The pyrolysis of alkylaromatics has been extensively investigated by researchers [42] [52] [38] [53]. The kinetic data from this literature reveals that the mole percent conversion of the alkylaromatic model compounds at a process severity similar to the current experimental conditions varies from 20 to 99 percent. Smith and Savage [42] have shown that the reactivity of polycyclic alkylaromatics has a dependence on alkyl chain length. As shown in Figure 4.16, the conversion of alkylpyrene during pyrolysis at 400°C and 120 minutes sharply increases as the chain length increases from one to five, after which the chain length plays a minor role in its overall reactivity. Figure 4.17 [49] shows the reaction network for the pyrolysis of dodecylpyrene. Due to its multi-ring aromatic structure attached to an alkyl chain, dodecylpyrene resembles the polycyclic alkylaromatic moieties present in heavy oil. It is known from the NMR carbon-type data that the maximum value for the average aromatic carbon cluster size in the residue fraction is 22 or 4-5 aromatic rings. Dodecylpyrene reacts by two pathways which are different due to the position of thermal cleavage of C-C bonds

Model Compounds	Abbreviations	Arrhenius Parameters		First Order Rate Constant (s-1)		Conversion (mole%)	
		A_o (s-1)	E_a (kcal/mol)	415°C	420°C	415°C	420°C
1,3-Diarylpropanes						30 min	
2-(3-phenylpropyl)-naphthalene	PPN			93.4 mole% conversion at time = 31 min and reaction temp of 400°C			
1,3-bis(1-pyrene)-propane	BPP			100 mole% conversion at time = 30 min and reaction temp of 365°C			
Hydroaromatics							
Tetralin	T			2.0 wt% conversion at time = 120 min and reaction temp of 450°C			
2-ethyl tetralin	2ET	5.0E+012	-53.5	5.1E-06	6.7E-06	8.8%	11.4%
2-dodecyl-9,10-dihydro-phenanthrene	DDPh	4.0E+013	-54.5	1.9E-04	2.6E-04	29.6%	37.4%
Polycyclic naphthenes							
Hexyl Cyclohexane	HXC	3.8E+013	-56.2	5.4E-05	7.2E-05	9.2%	12.2%
heptyl cyclohexane	HPC	5.0E+015	-62.6	6.6E-05	9.1E-05	11.1%	15.2%
1-decylperhydropyrene	1-DPP	3.5E+000	-42.9	8.4E-05	1.1E-04	14.0%	17.3%
decylcyclohexane	DC	1.0E+016	-62.6	1.3E-04	1.8E-04	21.0%	28.0%
tridecylcyclohexane	TDC	4.0E+015	-61.3	1.3E-04	1.9E-04	21.6%	28.5%
Undecyldecalin	UDD	7.9E+010	-48.5	1.4E-04	1.7E-04	21.6%	26.7%
octylperhydrochrysene	2-OPC	8.7E+013	-55.9	1.5E-04	2.1E-04	24.1%	30.9%
1-dodecylperhydro-phenanthrene	1DPPh	1.0E+016	-62.4	1.5E-04	2.1E-04	23.9%	31.6%
dodecylcyclohexane	DDC	4.0E+011	-48.5	1.6E-04	2.0E-04	24.6%	30.6%
9-dodecylperhydro-anthracene	9-DDPA	3.2E+010	-44.7	2.0E-04	2.5E-04	30.3%	38.7%
9-dodecylperhydro-phenanthrene	9DPPh	2.5E+010	-44.2	2.3E-04	2.9E-04	33.9%	40.7%
Polycyclic aromatics							
Unndecylnaphthalene	UDN	3.5E+014	-58.1	1.2E-04	1.6E-04	19.3%	25.3%
2-butylnaphthalene	2-BN	4.8E+020	-77.0	1.6E-04	2.5E-04	25.5%	35.8%
2-dodecylphenanthrene	2-DDH	1.2E+016	-62.4	1.9E-04	2.6E-04	28.9%	37.7%
Pentadecylbenzene	PDB	1.1E+014	-55.5	2.7E-04	3.6E-04	38.4%	47.7%
Octylchrysene	6-OC	5.6E+012	-51.2	3.0E-04	3.9E-04	41.7%	50.7%
Dodecylpyrene	DDP	3.9E+016	-62.3	6.6E-04	9.1E-04	69.4%	80.7%
3-hexylperylene	3-HP	2.3E+009	-30.2	7.8E-04	9.6E-04	75.6%	82.4%
Dodecylanthracene	9-DDA	5.3E+005	-26.4	2.1E-03	2.5E-03	97.8%	98.8%

Figure 4.15: Percentage Conversion of Model Compounds [29] [49] [40] [43] [50] [51]

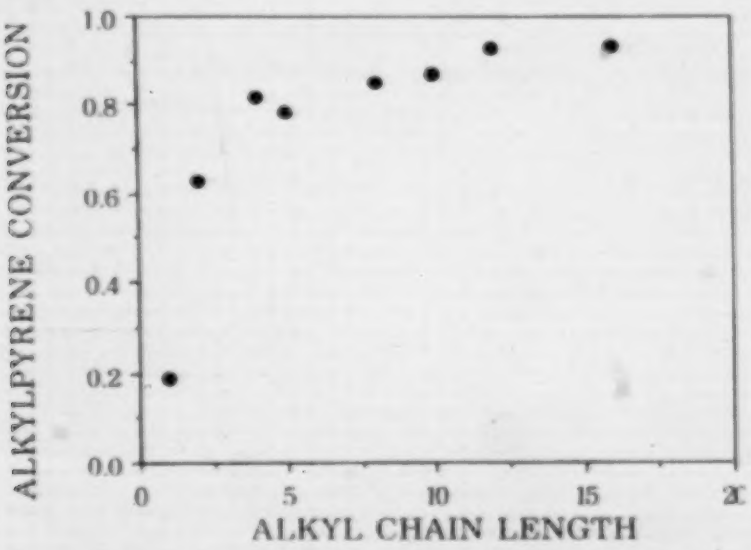

Figure 4.16: Effect of Chain length on Alkylpyrene Conversion [42]

at the ring. The side chain in pathway 1 breaks at the β position, while in pathway 2 breaks off at the strong aryl-alkyl α position. The first pathway is also analogous to the alkylbenzene pyrolysis. Different mechanisms have been proposed to explain the second pathway which involves the breaking of a strong alkyl-aryl bond, but irrespective of the pathways involved the kinetics and reaction network of polycyclic alkylaromatic pyrolysis indicates that these species are the most reactive species under mild conditions, their reactivity depends upon the length of alkyl chains and they react to form different lighter pseudo-components depending upon the length of the alkyl chain and the cluster size of the aromatic ring.

Polycyclic Alkylcycloparaffins

Model compounds representative of the polycyclic alkylcycloparaffins moieties in oil have also been studied for their pyrolysis behavior [34] [43] [45] [39]. Under identical reaction conditions, the mole percent conversion of these model compounds varies from 10 to 40 percent, having lower kinetic constants at similar temperatures than their polycyclic alkylaromatics equivalents. Major reaction products are produced

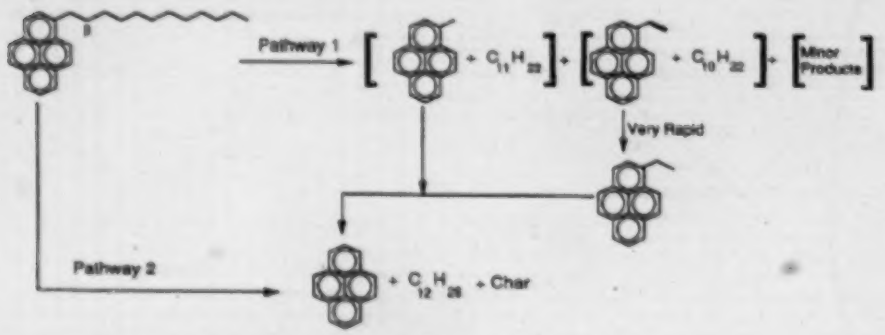

Figure 4.17: Pyrolysis Pathways for DDP [49]

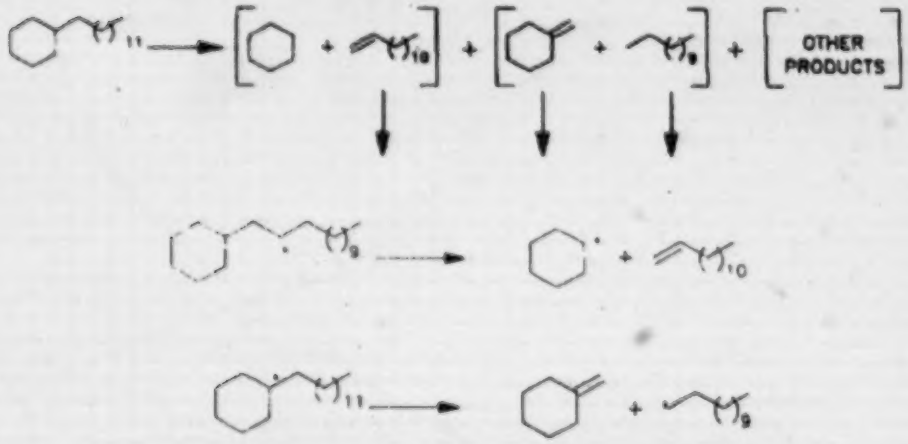

Figure 4.18: Pyrolysis Pathways for TDC [50]

by dealkylation at or near the ring and very little dehydrogenation is observed at identical reaction severity as seen in Figure 4.18 [50] and Figure 4.19 [43].

Savage et al. [43] have shown that the reactivity of polycyclic alkylcycloparaffins increases with the chain length and number of cycloparaffin rings.

1,3-Diarylalkanes

α,ω-Diphenylalkanes are relevant model compounds to represent polyaromatic species linked by paraffin chains in heavy oils [40]. The kinetic data of 1,3-diarylpropanes reveals that conversion of 2-(3-phenylpropyl)-naphthalene (PPN) is around

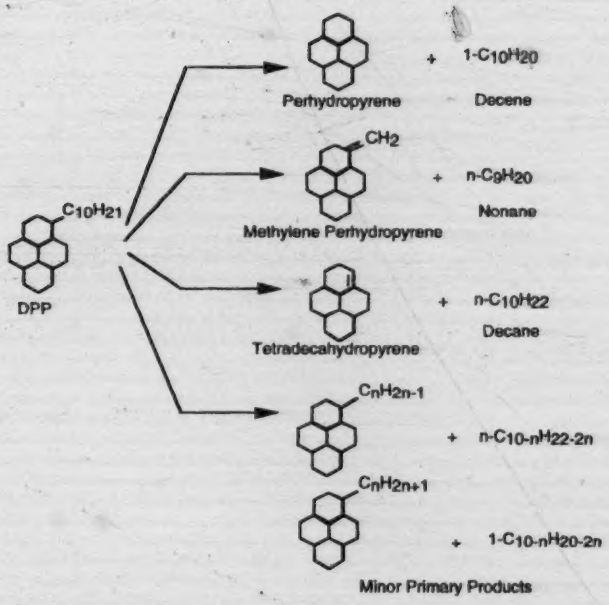

Figure 4.19: Pyrolysis Pathways for DPP [43]

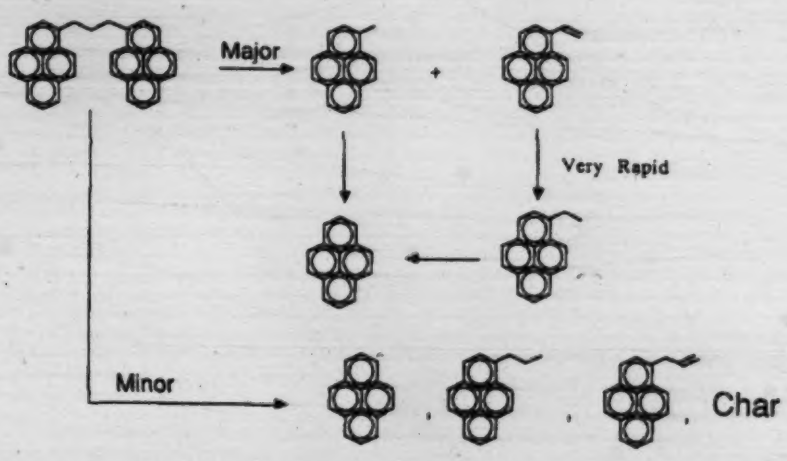

Figure 4.20: Pyrolysis Pathways for BPP [40]

94 percent under reaction conditions similar to the experimental, while that of 1,3-bis(1-pyrene)propane (BPP) is 100 percent at much milder conditions of 365°C and time of 31 minutes. Figure 2.9 showed the pyrolysis pathways of 2-(3-phenylpropyl)-naphthalene (PPN). PPN is also found more reactive than diphenylpropane under similar reaction conditions. The pyrolysis of 1,3-bis(1-pyrene)propane (BPP) is an example of a residue molecule converting to other residue molecules after thermal cleavage of aliphatic linkage as seen in Figure 4.20. The reaction products are produced by cleavage of C-C bond at the aryl-alkyl position or at other positions near the ring. The difference between the pyrolysis pathways of PPN and BPP is that the strong aryl-alkyl bond breaks only in the BPP pyrolysis. Various mechanisms are proposed to explain the cleavage of alkyl-aryl bond.

Depending upon the cluster size of the aromatic rings attached by paraffin chain, the pyrolysis products of 1,3-diarylalkanes might be a gasoil or residue fraction molecule.

Hydroaromatics

The presence of the α-to-aromatic cycloparaffins in the NMR data of the pseudo-components points to the existence of the hydroaromatic and alkylhydroaromatic

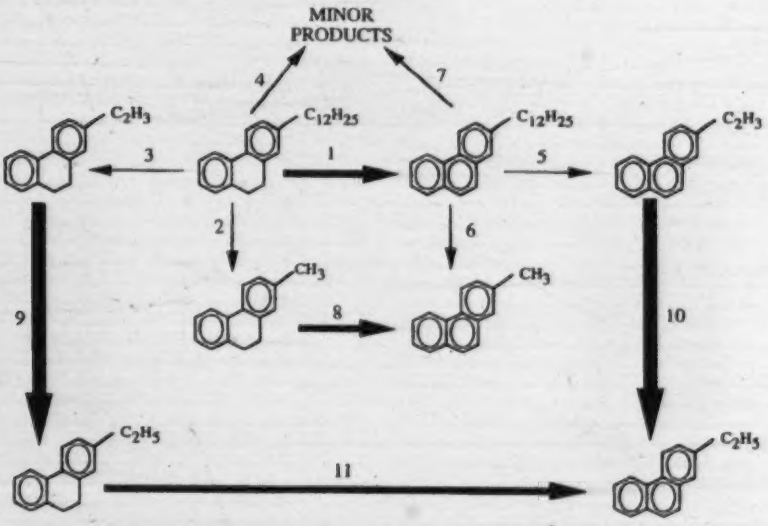

Figure 4.21: Pyrolysis Pathways for DDPh [29]

moieties in the oil. The kinetic data of these different model compounds indicate mole percent conversion of around 40 percent for 2-dodecyl-9,10-dihydrophenanthrene [29], 10 percent for 2-ethyltetralin [50] and around 1 percent for tetralin [51] at similar reaction severity. This indicates that polycyclic hydroaromatic moieties with long alkyl chains are more reactive. Figure 4.21 shows the reaction network for 2-dodecyl-9,10-dihydrophenanthrene (DDPh). At the experimental severity, the dehydrogenation pathway is the major one with a selectivity of 80-90 percent and only a small amount of other products are formed because of the side chain cleavage. But dehydrogenation of hydroaromatics alone would not lead to the conversion of residue fraction molecules like DDPh to lighter pseudo-components and thus this reaction would not contribute to residue conversion.

Figure 4.22 shows the pyrolysis pathways for 2-ethyltetralin (2ET) where naphthalene along with dialin form the major products. The dehydrogenation of the naphthenic ring seems to be the prominent reaction.

Thus, in the hydroaromatics pyrolysis, under the visbreaking conditions used, the major reaction pathway is the dehydrogenation of the naphthenic ring. The cleavage

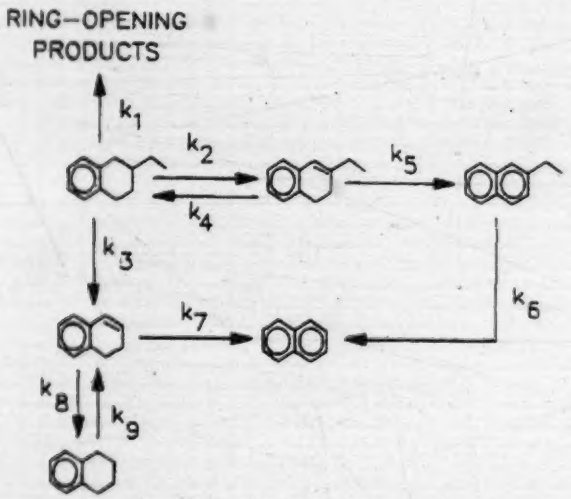

Figure 4.22: Pyrolysis Pathways for 2ET [50]

of the side chain at or near the ring is a minor pathway and does not contribute significantly to residue conversion to lighter pseudo-components.

4.2.5 Major Reactions during Visbreaking

From the pyrolysis studies of model compounds, it can be concluded that the polycyclic alkylaromatics are the most reactive species responsible for the residue conversion under visbreaking conditions, followed by the polycyclic cycloparaffins. The data in the work suggest that the cycloparaffin ring opening as well as the aromatic ring opening does not happen in the visbreaking conditions. Also, aromatization of paraffin chains does not occur under the existing conditions. Among the cycloparaffins, only the hydroaromatics get dehydrogenated to aromatics. The main reaction pathway for the conversion of residue to distillates during visbreaking is that of the cleavage of side chains.

Side Chain Cleavage

The average chain length in the residue fraction decreases in all feeds, with the exception of Kern River, during visbreaking as seen in Figure 4.8. The maximum

decrease in chainlength is observed in Athabasca and Kuwait heavy oil. With the decrease of the side chain length, the chain midsection carbon in residue also decreases and the percent decrease can be correlated to the percent residue conversion. The oil experiencing the maximum conversion has the maximum percent decrease of chain midsection carbon.

Cycloparaffin Dehydrogenation

The molar sum of aromatic and cycloparaffin carbon-types in the oils remains the same before and after cracking, with an error ranging from 3 to 9 percent. The conservation of moles of the aromatic and the naphthenic carbon-types in the oils before and after cracking implies that the rings do not get destroyed or formed; only the naphthenic rings are dehydrogenated to aromatics. Since the dehydrogenation is accompanied by the increase of boiling point and density, this does not lead to the formation of the lighter distillates.

Chapter 5

Model Development and Results

The main objective of this study is to develop a mathematical model, which is based on the principles of reaction chemistry and is able to predict the product yield of different fractions like gas, naphtha, gasoil, residue and coke after visbreaking of heavy oils at a single reaction severity. The six heavy oils chosen for the study are from different geographic regions of the world and are of different chemical nature. The basic assumption for the model is that at this severity, there are no secondary cracking reactions. It is also believed that most molecules in the feed pseudo-components do not react and for the most part, only one bond is broken for those that react.

5.1 Model Development

5.1.1 Residue Conversion

The percent conversion during visbreaking from residue fraction (524°C+) to distillates involves cracking to lighter products whose boiling point falls in the gasoil (204-524°C), naphtha (-204°C) boiling range, or the gas range. From the model compound studies, the most important pathway for the conversion of heavy oils during visbreaking is the side chain cleavage. The higher the alkyl substitution at the aromatic and possibly the naphthenic rings, the higher is the reactivity. Also the C-S bonds in the chains are weaker than other aliphatic bonds and are important cleavage sites. Thus, the residue conversion should be dependent upon the number of alkyl substituted aromatic and cycloparaffinic carbon-types and the sulfide sites

in chains. Another factor that directly affects residue conversion is the chain length. It is known that the reactivity of alkylaromatic model compounds linearly increases with the chain length and then maximizes at chain length approaching 5 carbon atoms. Previous work [54] suggested that side-chain cleavage of cycloparaffin species is minor due to the small ring cluster sizes (mostly 1 to 2 rings). As the oils in this study have similar cycloparaffin cluster sizes, it is expected that cleavage of their side-chains will also have a lower contribution. This expectation was supported in that when the content of alkyl-substituted cycloparaffinic carbon was included in the Residue Reactivity Index calculation, the correlation with residue conversion was not as good. Consequently, the contents of alkyl-substituted aromatic and sulphidic carbon and average chain lengths results were consolidated through the formulation of a Residue Reactivity Index (RRI) as

$$RRI = (A \cdot B) + C \tag{5.1}$$

where A= content of alkyl substituted aromatic carbon (moles), B= min (1, Alkyl chain length/5) and C= content of α-to-sulfides (moles).

The residue weight percent conversion was found to correlate with RRI with a correlation coefficient (R^2) of 0.87 as shown in Figure 5.1. The method of calculation of errors is given in Appendix B. It is to be noted that Rubiales which shows the lowest residue conversion, has the least alkyl substitution of aromatics and the shortest chains. This appears to be the reason why there was low residue conversion despite a high aromatic content.

5.1.2 Coke Formation

Conradson carbon, otherwise known as the microcarbon residue (MCR) content of various asphaltenes has been found to be dependent on their NMR-derived aromatic carbon content. With the availability of detailed NMR and elemental data for pseudo-components of all feed and visbroken product, the MCR content of these oils was calculated as the sum of aromatic carbon of residue polars and asphaltenes. Figure 5.2 shows the comparison of the experimental and calculated MCR values of the different feed and products. The correlation coefficient for the data is 0.89.

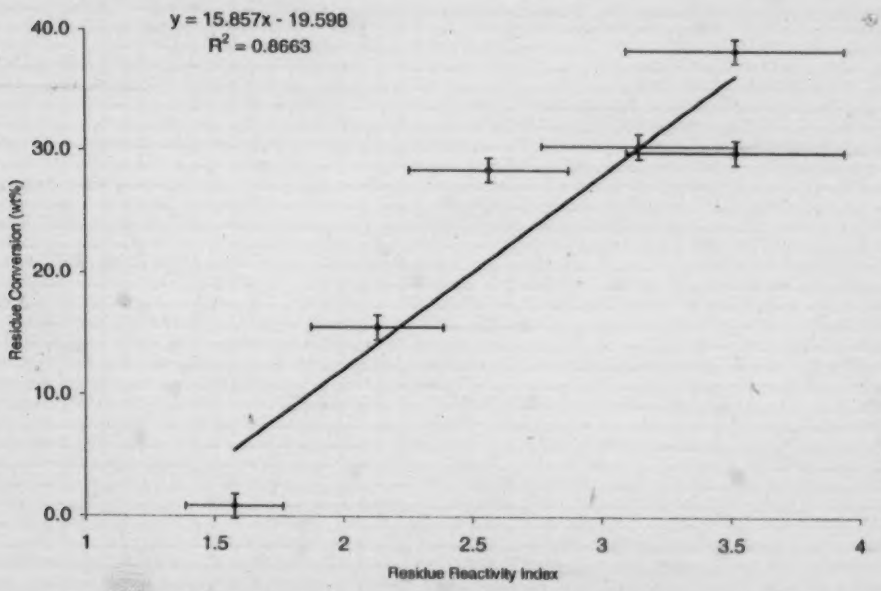

Figure 5.1: Residue Conversion vs RRI

The correlation is consistent with the hypothesis that after cracking of side chains, the aromatic carbon of polars and asphaltenes in the residue fraction are the major species that form coke.

Coke formation during visbreaking is measured by the toluene insolubles content of the visbroken product. The maximum visbreaking coke formation was observed in Rubiales, which has almost no residue conversion. Analysis of the contents of carbon-types of the residue asphaltenes shows that the number of moles of aromatic bridge and protonated aromatic (CH) carbon in the feed directly correlate with the contents of coke generated under the current conditions (correlation coefficient of 0.88) as seen in Figure 5.3. The contents of the total aromatic carbon do not correlate with the visbreaking coke as well. As coke formation under visbreaking conditions is close to the onset of coking, these results show that the least soluble species, the largest polyaromatics with the least alkyl substituents, will be the most likely to "fall out of solution" after one or two side chain bonds are broken.

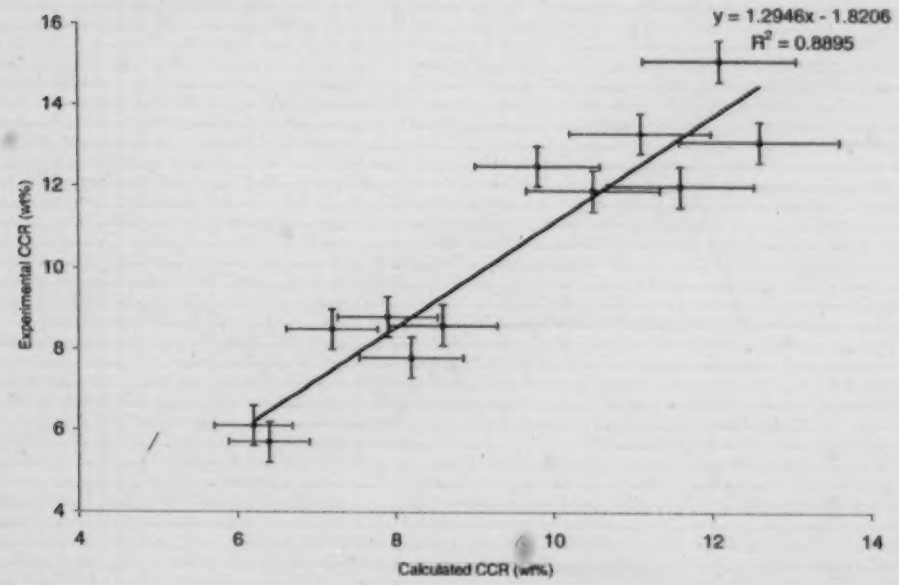

Figure 5.2: CCR vs Carbon-types

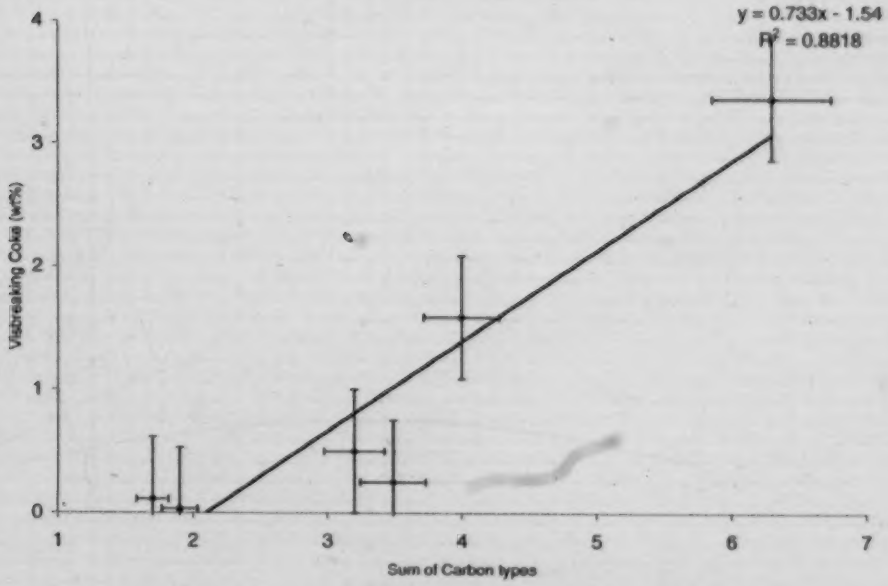

Figure 5.3: Visbreaking Coke vs. Carbon-types

5.1.3 Reaction Pathways

In the previous work [1], reaction pathways for the formation of lighter products during visbreaking of Athabasca bitumen were proposed and validated using carbon balances. The same reaction pathways have been adapted for the visbreaking of these different oils and used to predict the gas phase and naphtha products. The reaction pathways chosen indicate which carbon-types or groups of carbon-types in the feed are responsible for the production of methane, C2, C3+, naphtha aromatics, cycloparaffins and paraffins during the visbreaking reaction. The naphtha aromatics, paraffins and cycloparaffins combine together to form the total naphtha fraction. Naphtha aromatic carbon-types include aromatic bridges, alkylsubstituted aromatic carbon, aromatic CH and aromatic NS carbon-types. Naphtha paraffin carbon-types include paraffin chain, methyl aromatic, ethyl aromatic, propyl aromatic, diphenylmethane, methyl cycloparaffin, ethyl cycloparaffin, methyl branched chain, ethyl branched chain, butyl branched chain and the chain attachments carbon-types. Naphtha cycloparaffin carbon-types include cycloparaffin bridges, alkylsubstituted cycloparaffinic CH, cycloparaffinic CH2 and cycloparaffininc C(=CH2) carbon-types. Throughout the remaining chapter, different pseudo-components are referred by their acronyms. They are GO, GOS, GOA, GOP, RS, RA, RP, RAs representing gasoil, gasoil saturates, gasoil aromatics, gasoil polars, residue saturates, residue aromatics, residue polars, residue asphaltenes pseudo-components, respectively.

Reaction Pathway for Methane formation

$$(\mathrm{A+B})_{GO} + (\mathrm{A+B})_{RS} + (\mathrm{A+C})_{RA+RP+RAs} \Rightarrow \mathrm{Methane} \qquad (5.2)$$

where A= Methylcycloparaffin carbon (moles), B= Ethylaromatic carbon (moles) and C= Methylaromatic carbon (moles).

The methyl cycloparaffins in all pseudo-components contribute to the formation of methane through breaking off the methyl group that forms methane. Since the aromatics in gasoil and residue saturate have cluster size of 1-2 ring, the C-C bond at the β position in the ethylaromatics breaks off to release the methyl group and

form methane. However, in residue aromatics, polars and asphaltenes the aromatic cluster size is of the order of 3-4 ring and the alkyl-aryl bond breaks off preferentially in these polycyclic methylaromatics to release the methyl group that forms methane.

Reaction Pathway for C_2 formation

$$(A+B)_{GO} + (A+B)_{RS} + (A+C)_{RA+RP+RAs} \Rightarrow C2 \tag{5.3}$$

where A= Ethylcycloparaffin carbon (moles), B= Propylaromatic carbon (moles) and C= Ethylaromatic carbon (moles).

The ethyl cycloparaffins in all pseudo-components contribute to the formation of C2 through breaking off the ethyl group that forms C2. The logic for C2 formation remains the same as that of methane formation. Since the aromatic cluster size in gasoil and residue saturate are less than that of residuearomatics, polars and asphaltenes, the C-C bond at the β position breaks off, while the alkyl-aryl bond breaks off preferentially in the latter. Thus, propylaromatics are responsible for formation of C2 in gasoil and residue saturates while ethylaromatics are responsible in residue aromatics, polars and asphaltenes.

Reaction Pathway for C_{3+} formation

$$(A+B)_{GO} + (A+B)_{RS} + (A+B+C)_{RA+RP+RAs} \Rightarrow C3+ \tag{5.4}$$

where A= α-to-cycloparaffin carbon (moles), B= $\alpha\beta$-to-aromatic carbon (moles) and C= Propylaromatic carbon (moles).

The α-to-cycloparaffins in all pseudo-components contribute to the formation of C3+ through breaking off the side chains attached to cycloparaffin rings. The $\alpha\beta$-to-aromatics would similarly contribute to the formation of C3+ by breaking off the side chains either at the alkyl-aryl positions in polycylic alkylaromatics or at the β position in 1-2 ring aromatics. The propyl aromatics are included in the residue aromatics, polar and asphaltenes as breaking of the alkyl-aryl bond on propylaromatic would lead to formation of the propyl group that would form C3.

Reaction Pathway for Naphtha aromatics formation

$$(\text{A+B})_{GOA+GOP+RA+RP} \Rightarrow \text{Naphtha aromatics} \quad (5.5)$$

where A= Cycloparaffinic alkyl substituted CH carbon (moles)and B= Aromatic alkyl substituted carbon (moles),

The side chain cleavage is the main reaction behind residue conversion responsible for formation of different products during visbreaking. The aromatics are the most reactive species at such reaction conditions. Thus, the alkyl substituted aromatic carbon and the alkyl substituted cycloparaffinic CH in the polars and aromatic pseudo-components of gasoil and residue react (through bond breaking) to produce the naphtha aromatics. The residue asphaltenes have a much higher aromatic cluster size and would not produce naphtha aromatics. The residual aromatics (aromatic bridges, aromatic CH and aromatic NS carbon-types) in these fractions do not participate in the reaction to form naphtha aromatics and are not included in the reaction pathway. They, however contribute to the total aromaticity of reacting pseudo-components and thus play an important part in determining the amount of naphtha aromatics produced. The aromatic cluster size also plays a role in determining the reactivity of aromatic molecules of the reacting pseudo-components.

Reaction Pathway for Naphtha cycloparaffins formation

$$(\text{A+B})_{GOS+GOA+GOP+RS+RA+RP+RA_s} \Rightarrow \text{Naphtha cycloparaffins} \quad (5.6)$$

where A= Cycloparaffinic alkyl substituted CH carbon (moles) and B= Aromatic alkyl substituted carbon (moles).

The reasoning behind the pathway for the production of naphtha cycloparaffins is similar to that of naphtha aromatic. In the gasoil, the naphtha cycloparafins are produced from the saturates, aromatics and polars pseudo-components. All these three fractions have cycloparaffins and on reaction can contribute to naphtha cycloparaffins. In the residue, all four pseudo-components, saturates, aromatics, polars and asphaltenes contribute to naphtha cycloparaffins. The cycloparaffin cluster

size in asphaltene is 1-2 rings that makes the possibility of asphaltenes contributing to naphtha fraction on reaction. The side chain attached to the naphthenic and aromatic rings break off contributing to production of different products including cycloparaffins. Thus, the carbon-types responsible in all these pseudo-components are cycloparaffinic alkyl substituted CH and alkyl substituted aromatic carbon. The residual cycloparaffins (cycloparaffin bridges, cycloparaffinic CH2 and cycloparaffininc C(=CH2) carbon-types) in these fractions do not participate in the reaction to form naphtha cycloparaffins and are not included in the reaction pathway. They, however contribute to the total naphthenic content of reacting pseudo-components and thus play an important part in determining the amount of naphtha cycloparaffins produced. As in the case of formation of naphtha aromatics, the aromatic cluster size also plays a role in determining the reactivity of the reacting pseudo-components.

Reaction Pathway for Naphtha paraffins formation

$$(A+B)_{GOS+GOA+GOP+RS+RA+RP+RAs} \Rightarrow \text{Naphtha paraffins} \qquad (5.7)$$

where A= Cycloparaffinic alkyl substituted CH carbon (moles) and B= Aromatic alkyl substituted carbon (moles).

The logic behind the pathway for naphtha paraffin production is the same as that of naphtha cycloparaffins. The pseudo-components responsible are gasoil saturates, polars and aromatics and residue saturates, polars, aromatics and asphaltenes. The reacting carbon-types included are cycloparaffininc alkyl substituted CH and alkyl substituted aromatic carbon. The paraffin chain ends are the amount of the paraffin chains that terminate in the paraffin group and are akin to residual components. Once the side chain attached to aromatic and naphthenic rings break off, the paraffin chain ends contribute to the naphtha paraffins. These fractions do not participate in the reaction to form naphtha paraffins and are not included in the reaction pathway. They, however contribute to the total paraffinic content of reacting pseudo-components and thus play an important part in determining the amount of naphtha paraffins produced. As in the case of naphtha aromatics and cycloparaffins formation, the aromatic cluster size also plays a role in determining the reactivity of

the reacting pseudo-components.

The reaction pathways indicate the carbon-types that react to form gas and naphtha components. The prediction of the amount of gas and naphtha components produced during visbreaking, is done by building product correlations for different pseudo-components. The feed carbon-types responsible for the formation of gas and naphtha products and the aromatic cluster size are added together using relative ***weighting factors*** to form a ***weighted sum of model parameters***. This ***weighted sum of model parameters*** is correlated with the moles of carbon-types produced in gas and naphtha fractions. The ***weighting factors*** are calculated based on ***Model rules***.

5.1.4 Model rules

The ***Model rules*** are formulated based on the knowledge gathered from the model compound pyrolysis chemistry and apply to all pseudo-components.

Rule 1:

> The reactivity of alkyl substituted cycloparaffin CH is 60 percent of the reactivity of the alkyl substituted aromatic carbon. This is because the alkyl substituted aromatic carbon is the most reactive species in oil during visbreaking.

Rule 2:

> The propensity of gasoil to convert to gas and gasoil saturates to convert to naphtha is 10 percent of the propensity of the residue fraction (aromatics, polars and asphaltenes) to convert to gas and naphtha. This is because the composite gasoil and the gasoil saturates have lower aromatic content and being smaller, have smaller aromatic cluster size, both of which lead to lower reactivity.

Rule 3:

> The propensity of gasoil aromatics to convert to naphtha is 30 percent of the propensity of residue aromatics and polars to convert to naphtha.

This is because the gasoil aromatics molecules are smaller and so have smaller aromatic cluster size leading to lower reactivity.

Rule 4:

The propensity of residue saturates to convert to gas and naphtha is 30 percent of the propensity of residue aromatics, polars and asphaltenes to convert to gas and naphtha. This is because the residue saturates have lower aromatic content which makes them less reactive.

Rule 5:

The propensity of residue asphaltenes to convert to gas is equal to the propensity of residue aromatics and polars to convert to gas. The propensity of residue asphaltenes to convert to naphtha is 50 percent of the propensity of residue aromatics and polars to convert to naphtha. This is because the asphaltenes with their shorter side chains are more likely to produce gas than naphtha.

Rule 6:

The residual aromatics are the aromatic carbon-types other than the alkyl substituted aromatic carbon. The residual cycloparaffins are the cycloparaffinic carbon-types other than the cycloparaffinic alkyl substituted CH carbon. The paraffin chain ends are analogous to the residual paraffins. Thus the residual components are primarily the unreacted species during visbreaking. But they add to the aromatic or naphthenic or paraffinic nature of the reacting pseudo-components and thus play an important part in determining the quantity of naphtha aromatics, cycloparaffins and paraffins produced. Therefore, the residual aromatics, cycloparaffins and paraffins are considered twice as responsible as the alkyl substituted aromatic carbon for the production of naphtha aromatics, naphtha cycloparaffins and naphtha paraffins respectively.

Rule 7:

> The role of aromatic cluster size in determining the reactivity is less than that of alkyl aromatic substitution and the length of side chains. The effect of cluster size is thus considered as 15 percent of that of the aromatic alkyl substituted carbon in determining reactivity.

The following section shows the calculation of the ***weighted sum of model parameters*** for different pseudo-components in gas and naphtha fraction, produced during visbreaking. The product correlation is built by calculating the ***weighted sum of model parameters*** for each of the six oils and then correlating with the amount of pseudo-component produced.

5.1.5 Product Correlations for Gas Formation

The model parameters include the reacting carbon-types in feed which are shown in the reaction pathways, the unreacted carbon-types or the residual components and the aromatic cluster size. The weighted sum of model parameters is the sum of the product of different model parameters and their weighting factors. The calculation of weighting factors is done by attributing a base reactivity of 1 to a particular feed carbon-type and then calculating the other weighting factors using the model rules. The weighting factors signify the relative importance of different sources that produce a particular pseudo-component through a reaction pathway. For gas phase correlations, the data for visbreaking of Shengli was not used. This is because the Shengli, which is an aliphatic heavy oil with saturates of 42.9 percent, shows higher gas make than the aromatic heavy oils like Kuwait (saturates=27.4 percent.) and Kern River (saturates=28.9 percent.). It has been observed [19] [21] [24] that paraffinic oils have lower gas make than the aromatic oils, and therefore Shengli data is incorrect.

Methane Formation

The methane formed after visbreaking is correlated with the weighted sum of model parameters calculated for all feeds. It is given as:

Model Parameters	Weighting factors	Calculation	Rule
Methyl Aromatics $_{RAs}$	$a_1 = 1$		Base reactivity
Methyl Aromatics $_{RP}$	$a_2 = 1$	$= a_1$	Resid polars same as asphaltenes
Methyl Aromatics $_{RA}$	$a_3 = 1$	$= a_1$	Resid aromatics same as asphaltenes
Methyl Cycloparaffins $_{RAs}$	$a_4 = 0.6$	$= 0.6 \times a_1$	Cycloparaffins is 60% of aromatics: Rule 1
Methyl Cycloparaffins $_{RP}$	$a_5 = 0.6$	$= 0.6 \times a_2$	Cycloparaffins is 60% of aromatics: Rule 1
Methyl Cycloparaffins $_{RA}$	$a_6 = 0.6$	$= 0.6 \times a_3$	Cycloparaffins is 60% of aromatics: Rule 1
Ethyl Aromatics $_{RS}$	$a_7 = 0.3$	$= 0.3 \times a_3$	Resid saturates is 30% of resid aromatics: Rule 4
Methyl Cycloparaffins $_{RS}$	$a_8 = 0.18$	$= 0.6 \times a_7$	Cycloparaffins is 60% of aromatics: Rule 1
Ethyl Aromatics $_{GO}$	$a_9 = 0.1$	$= 0.1 \times a_3$	Gasoil is 10% of resid aromatics: Rule 2
Methyl Cycloparaffins $_{GO}$	$a_{10} = 0.06$	$= 0.6 \times a_9$	Cycloparaffins is 60% of aromatics: Rule 1

Figure 5.4: Weighting Factors for Methane Formation

$$\text{Weighted sum of model parameters} = a_1 \cdot C_{RAs} + a_2 \cdot C_{RP} + a_3 \cdot C_{RA} + a_4 \cdot A_{RAs} + a_5 \cdot A_{RP} + a_6 \cdot A_{RA} + a_7 \cdot B_{RS} + a_8 \cdot A_{RS} + a_9 \cdot B_{GO} + a_{10} \cdot A_{GO}$$

where A= Methylcycloparaffin carbon (moles) B= Ethylaromatic carbon (moles) and C= Methylaromatic carbon (moles).
The calculation of "weighting factors" is done as per the "model rules" as is shown in Figure 5.4. Figure 5.5 shows the correlation with a correlation coefficient of 0.92.

C_2 Formation

C_2 formed after visbreaking is correlated with the weighted sum of model parameters calculated for all feeds. It is given as:

$$\text{Weighted sum of model parameters} = b_1 \cdot C_{RAs} + b_2 \cdot C_{RP} + b_3 \cdot C_{RA} + b_4 \cdot A_{RAs} + b_5 \cdot A_{RP} + b_6 \cdot A_{RA} + b_7 \cdot B_{RS} + b_8 \cdot A_{RS} + b_9 \cdot B_{GO} + b_{10} \cdot A_{GO}$$

where A= Ethylcycloparaffin carbon (moles) B= Propylaromatic carbon (moles) and C= Ethylaromatic carbon (moles).

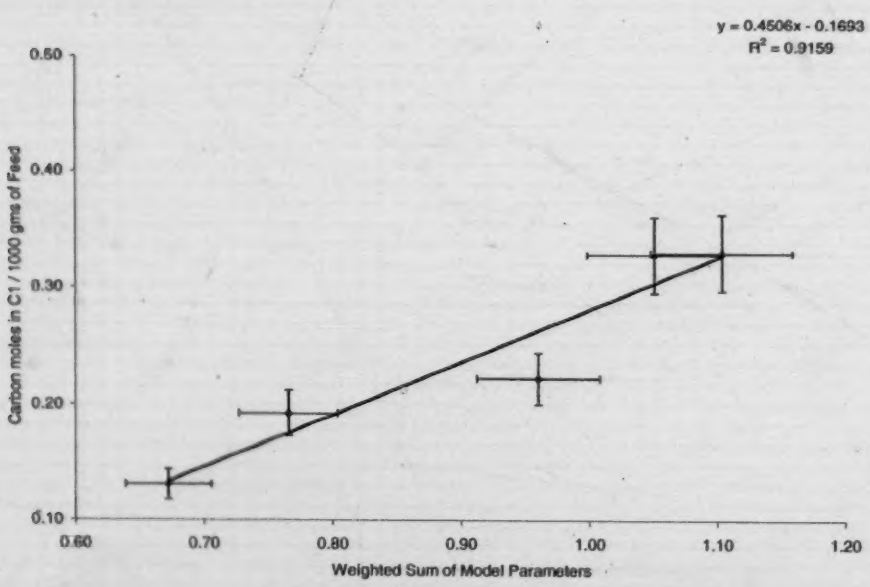

Figure 5.5: Carbon moles in CH4 vs Weighted sum of model parameters

Figure 5.6 shows the calculation of weighting factors as per the model rules. Figure 5.7 shows the correlation with a correlation coefficient of 0.66.

C_3+ Formation

C_3+ formed after visbreaking is correlated with the weighted sum of model parameters calculated for all feeds. It is given as:

$$\begin{aligned}\text{Weighted sum of model parameters} = {} & c_1 \cdot C_{RAs} + c_2 \cdot B_{RAs} + c_3 \cdot C_{RP} + c_4 \cdot B_{RP} \\ & + c_5 \cdot C_{RA} + c_6 \cdot B_{RA} + c_7 \cdot A_{RAs} + c_8 \cdot A_{RP} + c_9 \cdot A_{RA} + c_{10} \cdot B_{RS} \\ & + c_{11} \cdot A_{RS} + c_{12} \cdot B_{GO} + c_{13} \cdot A_{GO}\end{aligned}$$

where A= α-to-cycloparaffin carbon (moles) B= $\alpha\beta$-to-aromatic carbon (moles) and C= Propylaromatic carbon (moles).

The weighting factors are calculated as per the model rules and are shown in Table 5.8. Figure 5.9 shows the result of the correlation and the correlation coefficient

Model Parameters	Weighting factors	Calculation	Rule
Ethyl Aromatics $_{RAs}$	$b_1 = 1$		Base reactivity
Ethyl Aromatics $_{RP}$	$b_2 = 1$	$= b_1$	Resid polars same as asphaltenes
Ethyl Aromatics $_{RA}$	$b_3 = 1$	$= b_1$	Resid aromatics same as asphaltenes
Ethyl Cycloparaffins $_{RAs}$	$b_4 = 0.6$	$= 0.6 \times b_1$	Cycloparaffins is 60% of aromatics: Rule 1
Ethyl Cycloparaffins $_{RP}$	$b_5 = 0.6$	$= 0.6 \times b_2$	Cycloparaffins is 60% of aromatics: Rule 1
Ethyl Cycloparaffins $_{RA}$	$b_6 = 0.6$	$= 0.6 \times b_3$	Cycloparaffins is 60% of aromatics: Rule 1
Propyl Aromatics $_{RS}$	$b_7 = 0.3$	$= 0.3 \times b_3$	Resid saturates is 30% of resid aromatics: Rule 4
Ethyl Cycloparaffins $_{RS}$	$b_8 = 0.18$	$= 0.6 \times b_7$	Cycloparaffins is 60% of aromatics: Rule 1
Propyl Aromatics $_{GO}$	$b_9 = 0.1$	$= 0.1 \times b_3$	Gasoil is 10% of resid aromatics: Rule 2
Ethyl Cycloparaffins $_{GO}$	$b_{10} = 0.06$	$= 0.6 \times b_9$	Cycloparaffins is 60% of aromatics: Rule 1

Figure 5.6: Weighting Factors for C2 Formation

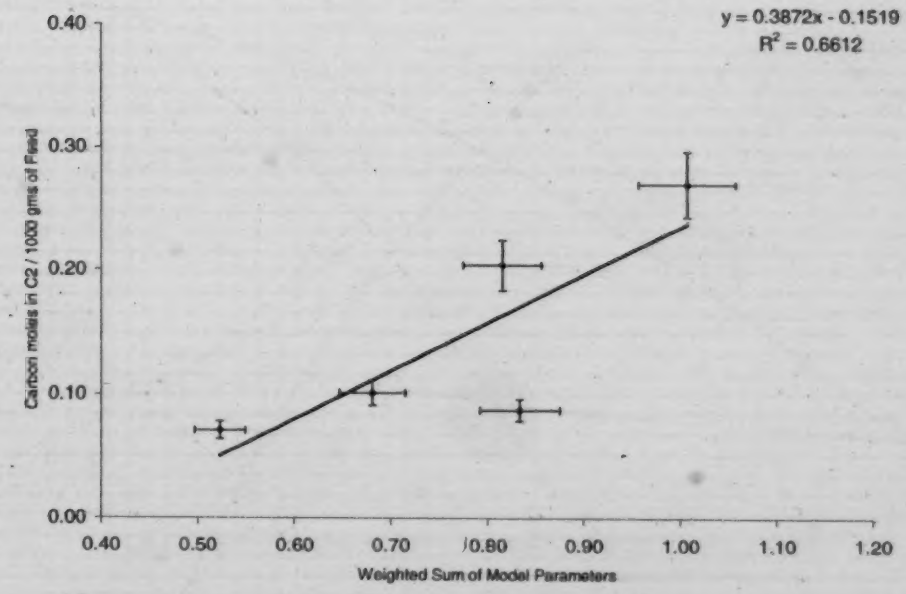

Figure 5.7: Carbon moles in C_2 vs Weighted sum of model parameters

Model Parameters	Weighting factors	Calculation	Rule
Propyl Aromatics $_{RAs}$	$c_1 = 1$		Base reactivity
αβ-to-aromatic $_{RAs}$	$c_2 = 1$	$= c_1$	Aromatics in residue asphaltenes, polar and aromatics fraction
Propyl Aromatics $_{RP}$	$c_3 = 1$	$= c_1$	
αβ-to-aromatic $_{RP}$	$c_4 = 1$	$= c_1$	
Propyl Aromatics $_{RA}$	$c_5 = 1$	$= c_1$	
αβ-to-aromatic $_{RA}$	$c_6 = 1$	$= c_1$	
α-to-cycloparaffin $_{RAs}$	$c_7 = 0.6$	$= 0.6 \times c_1$	Cycloparaffins is 60% of aromatics: Rule 1
α-to-cycloparaffin $_{RP}$	$c_8 = 0.6$	$= 0.6 \times c_1$	Cycloparaffins is 60% of aromatics: Rule 1
α-to-cycloparaffin $_{RA}$	$c_9 = 0.6$	$= 0.6 \times c_1$	Cycloparaffins is 60% of aromatics: Rule 1
αβ-to-aromatic $_{RS}$	$c_{10} = 0.3$	$= 0.3 \times c_6$	Resid saturates is 30% of resid aromatics: Rule 4
α-to-cycloparaffin $_{RS}$	$c_{11} = 0.18$	$= 0.6 \times c_{10}$	Cycloparaffins is 60% of aromatics: Rule 1
αβ-to-aromatic $_{GO}$	$c_{12} = 0.1$	$= 0.1 \times c_6$	Gasoil is 10% of resid aromatics: Rule 2
α-to-cycloparaffin $_{GO}$	$c_{13} = 0.06$	$= 0.6 \times c_{12}$	Cycloparaffins is 60% of aromatics: Rule 1

Figure 5.8: Weighting Factors for C_3+ Formation

is 0.67. The lower values of correlation coefficient for C_2 and C_3+ formation are because of two reasons. The first being that there could be more experimental error in the collection and determination of the gas during the experiment given the lower yields of these gases. The second reason is that gas production may take place from sources not considered in the reaction pathways or due to some secondary cracking.

5.1.6 Product Correlations for Naphtha Formation

Formation of Naphtha Aromatics

The aromatic carbon-types produced during visbreaking are the difference between the aromatic carbon-types in product naphtha and those in feed naphtha. They are correlated with the weighted sum of model parameters calculated for all feeds and is given as:

$$\begin{aligned}\text{Weighted sum of model parameters} = {} & d_1 \cdot B_{RA} + d_2 \cdot B_{RP} + d_3 \cdot A_{RA} + d_4 \cdot A_{RP} \\ & + d_5 \cdot D_{RA} + d_6 \cdot D_{RP} + d_7 \cdot C_{RA} + d_8 \cdot C_{RP} + d_9 \cdot B_{GOA} + d_{10} \cdot B_{GOP} \\ & + d_{11} \cdot A_{GOA} + d_{12} \cdot A_{GOP} + d_{13} \cdot D_{GOA} + d_{14} \cdot D_{GOP} + d_{15} \cdot C_{GOA} \\ & + d_{16} \cdot C_{GOP}\end{aligned}$$

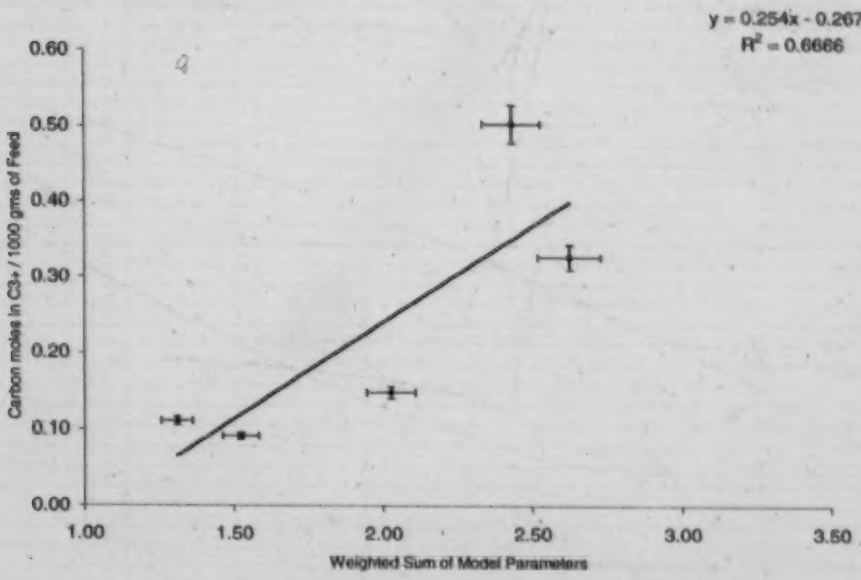

Figure 5.9: Carbon moles in C_3+ vs Weighted sum of model parameters

where A= Cycloparaffinic alkyl substituted CH carbon (moles), B= Aromatic alkyl substituted carbon (moles), C= Aromatic cluster size and D= Residual aromatic carbon (moles).

The weighting factors are shown in Figure 5.10. Figure 5.11 shows the correlation with a correlation coefficient of 0.85.

Formation of Naphtha Cycloparaffins

The cycloparaffin carbon-types produced during visbreaking are the difference between the cycloparaffin carbon-types in product naphtha and those in feed naphtha. It is correlated with the weighted sum of model parameters calculated for all feeds and is given as:

Model Parameters	Weighting factors	Calculation	Rule
Aromatic alkylsubstituted carbon $_{RA}$	$d_1 = 1$		Base reactivity
Aromatic alkylsubstituted carbon $_{RP}$	$d_2 = 1$	$= d_1$	Aromatics in residue polar and aromatics fraction
Cycloparaffin alkylsubstituted CH $_{RA}$	$d_3 = 0.6$	$= 0.6 \times d_1$	Cycloparaffins is 60% of aromatics: Rule 1
Cycloparaffin alkylsubstituted CH $_{RP}$	$d_4 = 0.6$	$= 0.6 \times d_2$	Cycloparaffins is 60% of aromatics: Rule 1
Residual Aromatics $_{RA}$	$d_5 = 2$	$= 2 \times d_1$	Residual aromatics are twice of the aromatic alkylsubs. C: Rule 6
Residual Aromatics $_{RP}$	$d_6 = 2$	$= 2 \times d_2$	Residual aromatics are twice of the aromatic alkylsubs. C: Rule 6
Aromatic cluster size $_{RA}$	$d_7 = 0.15$	$= 0.15 \times d_1$	Aromatic cluster size is 15% of the aromatic alkylsubs. C: Rule 7
Aromatic cluster size $_{RP}$	$d_8 = 0.15$	$= 0.15 \times d_2$	Aromatic cluster size is 15% of the aromatic alkylsubs. C: Rule 7
Aromatic alkylsubstituted carbon $_{GOA}$	$d_9 = 0.3$	$= 0.3 \times d_1$	Gasoil aromatics is 30% of resid aromatics: Rule 3
Aromatic alkylsubstituted carbon $_{GOP}$	$d_{10} = 0.3$	$= 0.3 \times d_2$	Gasoil aromatics is 30% of resid aromatics: Rule 3
Cycloparaffin alkylsubstituted CH $_{GOA}$	$d_{11} = 0.18$	$= 0.6 \times d_9$	Cycloparaffins is 60% of aromatics: Rule 1
Cycloparaffin alkylsubstituted CH $_{GOP}$	$d_{12} = 0.18$	$= 0.6 \times d_{10}$	Cycloparaffins is 60% of aromatics: Rule 1
Residual Aromatics $_{GOA}$	$d_{13} = 0.6$	$= 2 \times d_9$	Residual aromatics are twice of the aromatic alkylsubs. C: Rule 6
Residual Aromatics $_{GOP}$	$d_{14} = 0.6$	$= 2 \times d_{10}$	Residual aromatics are twice of the aromatic alkylsubs. C: Rule 6
Aromatic cluster size $_{GOA}$	$d_{15} = 0.45$	$= 0.15 \times d_9$	Aromatic cluster size is 15% of the aromatic alkylsubs. C: Rule 7
Aromatic cluster size $_{GOP}$	$d_{16} = 0.45$	$= 0.15 \times d_{10}$	Aromatic cluster size is 15% of the aromatic alkylsubs. C: Rule 7

Figure 5.10: Weighting Factors for Naphtha Aromatics Formation

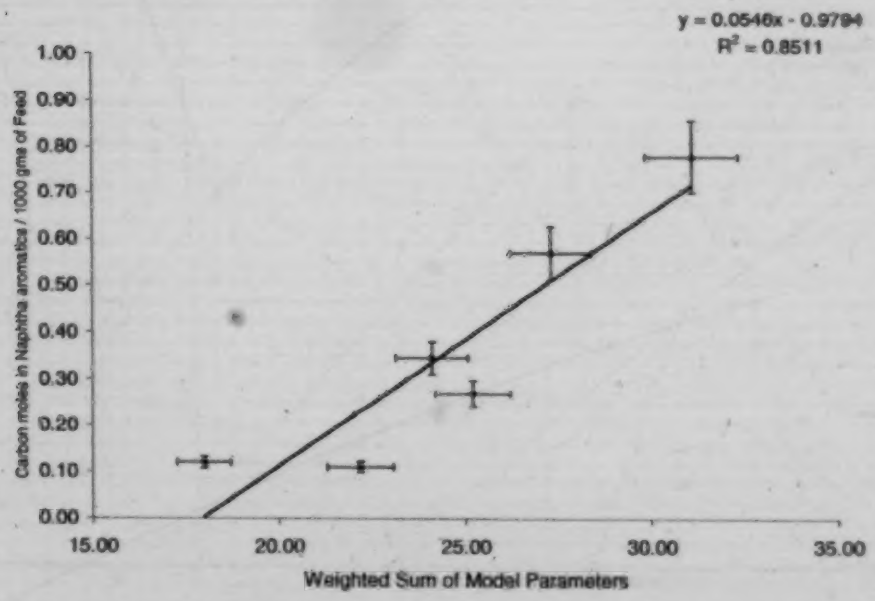

Figure 5.11: Product Naphtha aromatics vs Weighted sum of model parameters

$$\begin{aligned}\text{Weighted sum of model parameters} = {} & e_1 \cdot B_{RA} + e_2 \cdot B_{RP} + e_3 \cdot A_{RA} + e_4 \cdot A_{RP} \\ & + e_5 \cdot D_{RA} + e_6 \cdot D_{RP} + e_7 \cdot C_{RA} + e_8 \cdot C_{RP} + e_9 \cdot B_{GOA} + e_{10} \cdot B_{GOP} \\ & + e_{11} \cdot A_{GOA} + e_{12} \cdot A_{GOP} + e_{13} \cdot D_{GOA} + e_{14} \cdot D_{GOP} + e_{15} \cdot C_{GOA} \\ & + e_{16} \cdot C_{GOP} + e_{17} \cdot B_{RA_3} + e_{18} \cdot A_{RA_3} + e_{19} \cdot D_{RA_3} + e_{20} \cdot C_{RA_3} \\ & + e_{21} \cdot B_{RS} + e_{22} \cdot B_{GOS} + e_{23} \cdot A_{RS} + e_{24} \cdot A_{GOS} + e_{25} \cdot D_{RS} \\ & + e_{26} \cdot D_{GOS} + e_{27} \cdot C_{RS} + e_{28} \cdot C_{GOS}\end{aligned}$$

where A= Cycloparaffinic alkyl substituted CH carbon (moles), B= Aromatic alkyl substituted carbon (moles), C= Aromatic cluster size and D= Residual cycloparaffin carbon (moles).

Figure 5.12 shows the weighting factors used for the calculation. Figure 5.13 shows the correlation with a correlation coefficient of 0.85.

Model Parameters	Weighting factors	Calculation	Rule
Aromatic alkylsubstituted carbon $_{RA}$	$e_1 = 1$		Base reactivity
Aromatic alkylsubstituted carbon $_{RP}$	$e_2 = 1$	$= e_1$	Aromatics in residue polar and aromatics fraction
Cycloparaffin alkylsubstituted CH $_{RA}$	$e_3 = 0.6$	$= 0.6 \times e_1$	Cycloparaffins is 60% of aromatics: Rule 1
Cycloparaffin alkylsubstituted CH $_{RP}$	$e_4 = 0.6$	$= 0.6 \times e_2$	Cycloparaffins is 60% of aromatics: Rule 1
Residual Cycloparaffins $_{RA}$	$e_5 = 2$	$= 2 \times e_1$	Residual cycloparaffins are twice of the aromatic alkylsubs. C: Rule 6
Residual Cycloparaffins $_{RP}$	$e_6 = 2$	$= 2 \times e_2$	Residual cycloparaffins are twice of the aromatic alkylsubs. C: Rule 6
Aromatic cluster size $_{RA}$	$e_7 = 0.15$	$= 0.15 \times e_1$	Aromatic cluster size is 15% of the aromatic alkylsubs. C: Rule 7
Aromatic cluster size $_{RP}$	$e_8 = 0.15$	$= 0.15 \times e_2$	Aromatic cluster size is 15% of the aromatic alkylsubs. C: Rule 7
Aromatic alkylsubstituted carbon $_{GOA}$	$e_9 = 0.3$	$= 0.3 \times e_1$	Gasoil aromatics is 30% of resid aromatics: Rule 3
Aromatic alkylsubstituted carbon $_{GOP}$	$e_{10} = 0.3$	$= 0.3 \times e_2$	Gasoil aromatics is 30% of resid aromatics: Rule 3
Cycloparaffin alkylsubstituted CH $_{GOA}$	$e_{11} = 0.18$	$= 0.6 \times e_9$	Cycloparaffins is 60% of aromatics: Rule 1
Cycloparaffin alkylsubstituted CH $_{GOP}$	$e_{12} = 0.18$	$= 0.6 \times e_{10}$	Cycloparaffins is 60% of aromatics: Rule 1
Residual Cycloparaffins $_{GOA}$	$e_{13} = 0.6$	$= 2 \times e_9$	Residual cycloparaffins are twice of the aromatic alkylsubs. C: Rule 6
Residual Cycloparaffins $_{GOP}$	$e_{14} = 0.6$	$= 2 \times e_{10}$	Residual cycloparaffins are twice of the aromatic alkylsubs. C: Rule 6
Aromatic cluster size $_{GOA}$	$e_{15} = 0.45$	$= 0.15 \times e_9$	Aromatic cluster size is 15% of the aromatic alkylsubs. C: Rule 7
Aromatic cluster size $_{GOP}$	$e_{16} = 0.45$	$= 0.15 \times e_{10}$	Aromatic cluster size is 15% of the aromatic alkylsubs. C: Rule 7
Aromatic alkylsubstituted carbon $_{RAS}$	$e_{17} = 0.5$	$= 0.5 \times e_1$	Rule 5
Cycloparaffin alkylsubstituted CH $_{RAS}$	$e_{18} = 0.3$	$= 0.6 \times e_{17}$	Cycloparaffins is 60% of aromatics: Rule 1
Residual Cycloparaffins $_{RAS}$	$e_{19} = 1$	$= 2 \times e_{17}$	Residual cycloparaffins are twice of the aromatic alkylsubs. C: Rule 6
Aromatic cluster size $_{RAS}$	$e_{20} = 0.75$	$= 0.15 \times e_{17}$	Aromatic cluster size is 15% of the aromatic alkylsubs. C: Rule 7
Aromatic alkylsubstituted carbon $_{RS}$	$e_{21} = 0.3$	$= 0.3 \times e_1$	Resid saturates is 30% of resid aromatics: Rule 4
Aromatic alkylsubstituted carbon $_{GOS}$	$e_{22} = 0.1$	$= 0.1 \times e_1$	Gasoil is 10% of resid aromatics: Rule 2
Cycloparaffin alkylsubstituted CH $_{RS}$	$e_{23} = 0.18$	$= 0.6 \times e_{21}$	Cycloparaffins is 60% of aromatics: Rule 1
Cycloparaffin alkylsubstituted CH $_{GOS}$	$e_{24} = 0.06$	$= 0.6 \times e_{22}$	Cycloparaffins is 60% of aromatics: Rule 1
Residual Cycloparaffins $_{RS}$	$e_{25} = 0.6$	$= 2 \times e_{21}$	Residual cycloparaffins are twice of the aromatic alkylsubs. C: Rule 6
Residual Cycloparaffins $_{GOS}$	$e_{26} = 0.2$	$= 2 \times e_{22}$	Residual cycloparaffins are twice of the aromatic alkylsubs. C: Rule 6
Aromatic cluster size $_{RS}$	$e_{27} = 0.45$	$= 0.15 \times e_{21}$	Aromatic cluster size is 15% of the aromatic alkylsubs. C: Rule 7
Aromatic cluster size $_{GOS}$	$e_{28} = 0.015$	$= 0.15 \times e_{22}$	Aromatic cluster size is 15% of the aromatic alkylsubs. C: Rule 7

Figure 5.12: Weighting Factors for Naphtha Cycloparaffins Formation

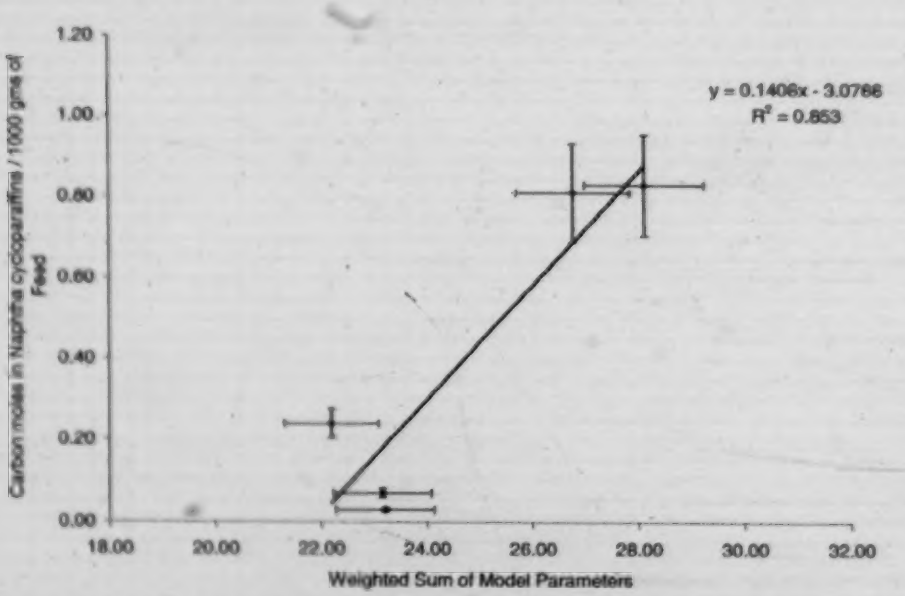

Figure 5.13: Product Naphtha Cycloparaffins vs Weighted sum of model parameters

Formation of Naphtha Paraffins

The paraffin carbon-types produced during visbreaking are the difference between the paraffin carbon-types in product naphtha and those in feed naphtha. It is correlated with the weighted sum of model parameters calculated for all feeds and is given as:

$$\begin{aligned}\text{Weighted sum of model parameters} = {} & f_1 \cdot B_{RA} + f_2 \cdot B_{RP} + f_3 \cdot A_{RA} + f_4 \cdot A_{RP} \\ & + f_5 \cdot D_{RA} + f_6 \cdot D_{RP} + f_7 \cdot C_{RA} + f_8 \cdot C_{RP} + f_9 \cdot B_{GOA} + f_{10} \cdot B_{GOP} \\ & + f_{11} \cdot A_{GOA} + f_{12} \cdot A_{GOP} + f_{13} \cdot D_{GOA} + f_{14} \cdot D_{GOP} + f_{15} \cdot C_{GOA} \\ & + f_{16} \cdot C_{GOP} + f_{17} \cdot B_{RA_3} + f_{18} \cdot A_{RA_3} + f_{19} \cdot D_{RA_3} + f_{20} \cdot C_{RA_3} \\ & + f_{21} \cdot B_{RS} + f_{22} \cdot B_{GOS} + f_{23} \cdot A_{RS} + f_{24} \cdot A_{GOS} + f_{25} \cdot D_{RS} \\ & + f_{26} \cdot D_{GOS} + f_{27} \cdot C_{RS} + f_{28} \cdot C_{GOS}\end{aligned}$$

where A= Cycloparaffinic alkyl substituted CH carbon (moles), B= Aromatic alkyl

substituted carbon (moles), C= Aromatic cluster size and D= Paraffin chain ends carbon (moles).

Figure 5.14 shows the weighting factors used for the calculation. Figure 5.15 shows the correlation and the correlation coefficient of 0.76.

5.1.7 Prediction of Gasoil and Residue Formation

The residue fraction after visbreaking is calculated from the percentage residue conversion of the feed. The percentage residue conversion is predicted using Residue Reactivity Index of the feed and Figure 5.1. The sum of naphtha paraffins, cycloparaffins and aromatics produced during visbreaking is the total naphtha produced. This is added to the quantity of feed naphtha to give the total product naphtha. The sum of methane, C_2 and C_3+ gives the total product gas. Then, the gasoil product is calculated by balance.

Model Parameters	Weighting factors	Calculation	Rule
Aromatic alkylsubstituted carbon $_{RA}$	$f_1 = 1$		Base reactivity
Aromatic alkylsubstituted carbon $_{RP}$	$f_2 = 1$	$= f_1$	Aromatics in residue polar and aromatics fraction
Cycloparaffin alkylsubstituted CH $_{RA}$	$f_3 = 0.6$	$= 0.6 \times f_1$	Cycloparaffins is 60% of aromatics: Rule 1
Cycloparaffin alkylsubstituted CH $_{RP}$	$f_4 = 0.6$	$= 0.6 \times f_2$	Cycloparaffins is 60% of aromatics: Rule 1
Paraffin Chain ends $_{RA}$	$f_5 = 2$	$= 2 \times f_1$	Paraffin chain ends are twice of the aromatic alkylsubs. C: Rule 6
Paraffin Chain ends $_{RP}$	$f_6 = 2$	$= 2 \times f_2$	Paraffin chain ends are twice of the aromatic alkylsubs. C: Rule 6
Aromatic cluster size $_{RA}$	$f_7 = 0.15$	$= 0.15 \times f_1$	Aromatic cluster size is 15% of the aromatic alkylsubs. C: Rule 7
Aromatic cluster size $_{RP}$	$f_8 = 0.15$	$= 0.15 \times f_2$	Aromatic cluster size is 15% of the aromatic alkylsubs. C: Rule 7
Aromatic alkylsubstituted carbon $_{GOA}$	$f_9 = 0.3$	$= 0.3 \times f_1$	Gasoil aromatics is 30% of resid aromatics: Rule 3
Aromatic alkylsubstituted carbon $_{GOP}$	$f_{10} = 0.3$	$= 0.3 \times f_2$	Gasoil aromatics is 30% of resid aromatics: Rule 3
Cycloparaffin alkylsubstituted CH $_{GOA}$	$f_{11} = 0.18$	$= 0.6 \times f_9$	Cycloparaffins is 60% of aromatics: Rule 1
Cycloparaffin alkylsubstituted CH $_{GOP}$	$f_{12} = 0.18$	$= 0.6 \times f_{10}$	Cycloparaffins is 60% of aromatics: Rule 1
Paraffin Chain ends $_{GOA}$	$f_{13} = 0.6$	$= 2 \times f_9$	Paraffin chain ends are twice of the aromatic alkylsubs. C: Rule 6
Paraffin Chain ends $_{GOP}$	$f_{14} = 0.6$	$= 2 \times f_{10}$	Paraffin chain ends are twice of the aromatic alkylsubs. C: Rule 6
Aromatic cluster size $_{GOA}$	$f_{15} = 0.45$	$= 0.15 \times f_9$	Aromatic cluster size is 15% of the aromatic alkylsubs. C: Rule 7
Aromatic cluster size $_{GOP}$	$f_{16} = 0.45$	$= 0.15 \times f_{10}$	Aromatic cluster size is 15% of the aromatic alkylsubs. C: Rule 7
Aromatic alkylsubstituted carbon $_{RAS/S}$	$f_{17} = 0.5$	$= 0.5 \times f_1$	Rule 5
Cycloparaffin alkylsubstituted CH $_{RAS}$	$f_{18} = 0.3$	$= 0.6 \times f_{17}$	Cycloparaffins is 60% of aromatics: Rule 1
Paraffin Chain ends $_{RAS}$	$f_{19} = 1$	$= 2 \times f_{17}$	Paraffin chain ends are twice of the aromatic alkylsubs. C: Rule 6
Aromatic cluster size $_{RAS}$	$f_{20} = 0.75$	$= 0.15 \times f_{17}$	Aromatic cluster size is 15% of the aromatic alkylsubs. C: Rule 7
Aromatic alkylsubstituted carbon $_{RS}$	$f_{21} = 0.3$	$= 0.3 \times f_1$	Resid saturates is 30% of resid aromatics: Rule 4
Aromatic alkylsubstituted carbon $_{GOS}$	$f_{22} = 0.1$	$= 0.1 \times f_1$	Gasoil is 10% of resid aromatics: Rule 2
Cycloparaffin alkylsubstituted CH $_{RS}$	$f_{23} = 0.18$	$= 0.6 \times f_{21}$	Cycloparaffins is 60% of aromatics: Rule 1
Cycloparaffin alkylsubstituted CH $_{GOS}$	$f_{24} = 0.06$	$= 0.6 \times f_{22}$	Cycloparaffins is 60% of aromatics: Rule 1
Paraffin Chain ends $_{RS}$	$f_{25} = 0.6$	$= 2 \times f_{21}$	Paraffin chain ends are twice of the aromatic alkylsubs. C: Rule 6
Paraffin Chain ends $_{GOS}$	$f_{26} = 0.2$	$= 2 \times f_{22}$	Paraffin chain ends are twice of the aromatic alkylsubs. C: Rule 6
Aromatic cluster size $_{RS}$	$f_{27} = 0.45$	$= 0.15 \times f_{21}$	Aromatic cluster size is 15% of the aromatic alkylsubs. C: Rule 7
Aromatic cluster size $_{GOS}$	$f_{28} = 0.015$	$= 0.15 \times f_{22}$	Aromatic cluster size is 15% of the aromatic alkylsubs. C: Rule 7

Figure 5.14: Weighting Factors for Naphtha paraffins Formation

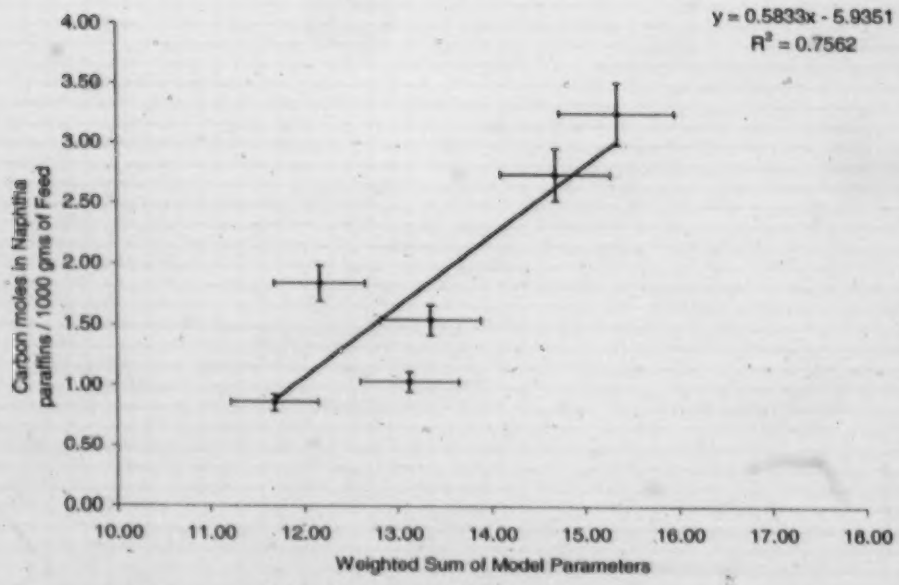

Figure 5.15: Product Naphtha paraffins vs Weighted sum of model parameters

Chapter 6

Model Use and Validation

6.1 Model Use

The end use of the model is to calculate the product yields from visbreaking of any global oil at the experimental severity. The calculation procedure for different sample calculations is shown in Appendix C.

- The first step is to calculate the residue conversion after visbreaking. This is done by calculating the Residue Reactivity Index of the feed oil. The Residue Reactivity Index is calculated using equation 5.1 with the use of alkyl substituted aromatic carbon-types, average chain length and α-to-sulfides carbon types in feed. The correlation in Figure 5.1 is used to calculate the percent residue conversion. After calculation of the percent residue conversion, the residue amount in the product can be calculated.

- The second step is to calculate the visbreaking coke formed and the CCR content of the feed. The sum of aromatic bridges and the aromatic CH carbon-types in asphaltenes in feed is calculated and the correlation in Figure 5.3 is used to calculate the percent visbreaking coke. The mass of aromatic carbon in residue polars and asphaltenes is calculated as percent of feed and is equal to the CCR content of the feed.

- The next step is to calculate the gas yield after visbreaking. The moles of carbon in methane produced is estimated using weighted sum of model parameters for methane formation and the correlation in Figure 5.5. The moles

of C_2 produced is estimated using weighted sum of model parameters for C_2 formation and the correlation in Figure 5.7 while the moles of C_3+ produced is estimated using weighted sum of model parameters for C_3+ formation and the correlation in Figure 5.9. After adding the moles of all carbon types from gas, its total weight is calculated. An estimated carbon weight percent of 65 is used for gas and the total weight of gas is calculated and expressed as percent of feed.

- After calculation of the gas make, the naphtha make is calculated. This is done by adding the moles of naphtha aromatic, naphtha paraffin and naphtha cycloparaffinic carbon-types. The naphtha aromatic carbon-types is estimated using weighted sum of model parameters for naphtha aromatics formation and the correlation in Figure 5.11. The naphtha paraffin carbon-types is estimated using weighted sum of model parameters for naphtha paraffin formation and the correlation in Figure 5.15. The naphtha cycloparaffinic carbon-types is estimated using weighted sum of model parameters for naphtha cycloparaffin formation and the correlation in Figure 5.13. After calculating the total moles of carbon-types in naphtha, the weight of the carbon-types is calculated and the percent weight carbon from the elemental analysis of feed naphtha is used to calculate the total weight of product naphtha. It is assumed here that the percent weight of carbon in feed and product naphtha remains the same. Once the weight of naphtha produced during visbreaking is found, it is added to the percent weight of feed naphtha to get the weight percent of product naphtha.

- With the calculation of the product yields of gas, naphtha and the residue fraction, the last step is to calculate the product gasoil by balance.

6.2 Model Validation

The model was developed using all the available six oils. The process of model validation would involve using the measured lab data of visbreaking for a *new* oil, use the model to predict the product yields from visbreaking of this oil and then calculate the prediction errors. But since the objective was to develop a rule-based

	Kuwait		
Yield (wt%)	Experimental	Predicted	Difference%
Gas	0.8	0.7	5.6
Naphtha	14.5	14.4	0.6
Gasoil	56.1	56.2	-0.2
Residue	28.6	28.7	-0.1
Feed CCR	8.61	9.39	-9.0
Visbreaking Coke	0.50	0.87	-72.6
	Kern River		
	Experimental	Predicted	Difference%
Gas	1.0	1.3	-33.2
Naphtha	5.1	3.5	31.3
Gasoil	65.6	63.3	3.5
Residue	28.3	31.9	-12.6
Feed CCR	7.82	8.91	-14.0
Visbreaking Coke	0.03	0.00	100.0
	Wolf Lake		
	Experimental	Predicted	Difference%
Gas	2.0	1.9	1.7
Naphtha	5.4	6.7	-23.6
Gasoil	56.0	59.9	-6.9
Residue	36.6	31.4	14.0
Feed CCR	12.50	10.71	14.3
Visbreaking Coke	0.25	1.17	-375.6

Figure 6.1: Model Predictions

model based on principles of reaction chemistry, the NMR carbon-type data from all six feeds was used in developing the model. Therefore, the model was validated by removing one dataset, re-estimating the correlation equations and then predicting the yields of the oil and calculating the percentage difference between the measured and predicted values. This process was repeated with three oils, Kuwait, Kern River, and Wolf Lake. Figure 6.1 summarizes the results of the validation exercise. The least errors are seen in Kuwait. The percentage difference between the predicted and measured values is very high in visbreaking coke due to the very little amount of visbreaking coke that was formed. The present modeling exercise emphasized on proposing and developing rule-based correlations and using them to predict the product yields. With the availability of more chemical kinetics data of the involved carbon-types, the existing model can be further improved.

Chapter 7

Conclusions and Future Work

7.1 Conclusions

This work presents a mathematical model of visbreaking using carbon-types present in feed oil. The model predicts residue conversion, coke formation and product yields on visbreaking. Since it has been built using six heavy oils from different parts of the world, it is expected to be robust enough to predict the visbreaking behavior of different types of oil.

The model input data includes the most extensive kind of NMR carbon-type analysis that has been performed on heavy oils. This analysis carried out at the National Centre for Upgrading Technology, Devon, Alberta, has helped to provide a much deeper insight into the chemistry of heavy oils involved and has made possible selection of model compounds that closely resemble different pseudo-components of these heavy oils. The pyrolysis pathways, the reaction mechanism and the kinetic information of these model compounds available in literature has helped to determine the carbon-types and the reactions that influence visbreaking the most. In the earlier work [1], visbreaking reaction pathways for Athabasca bitumen were proposed. These pathways have been improved and adapted to the NMR information from different oils. These pathways demonstrate the carbon-types in feed oil that act as possible sources for the production of new carbon-types during visbreaking. Through the use of *feed-independent* model rules, *weighting-factors* were developed, and then used to calculate different *weighted sum of model parameters* in these oils. These *weighted sum of model parameters* are analogous to the pool of reactants and have been

used to correlate percentage residue conversion, CCR make, visbreaking coke make and the make of lighter products, gas and naphtha, after visbreaking. From its ability to predict the visbreaking behavior of six different global oils, the model offers improved knowledge about the chemical reactivity of petroleum oils. It is found that the percentage conversion of a heavy oil during visbreaking is dependent on the alkyl substituted aromatic carbon, alkyl chain length and the α-to-sulphides in the residue fraction in feed. So the reactivity of an oil depends upon the the number of the side chains attached to its aromatic rings and the length of these side chains. The CCR content of a feed or a visbroken product is found equal to the weight of aromatic carbon in the residue polars and asphaltenes fraction. The visbreaking coke is directly dependent upon the quantity of the aromatic bridges and aromatic CH carbon-types in the residue asphaltenes fraction of the feed. The gas and naphtha is produced due to the cleavage of side chains on the aromatic and cycloparaffinic rings in gasoil and residue fraction. The side chains break off to produce smaller molecules that constitute gas and naphtha.

The use of reaction pathways and *feed-independent* model rules make this model rule-based. Earlier models used feed-specific kinetic parameters to predict visbreaking product yields and these kinetic parameters were calculated based on visbreaking pilot plant runs or lab scale pyrolysis experiments. The present model only makes use of the NMR carbon-type analysis, elemental analysis and distillation data of feed to predict its visbreaking product yields. Along with the prediction of visbreaking behavior of other oils, the model is successful in predicting the residue conversion, coke yield and other product yields for an *unconventional* oil like Rubiales, which baffles by showing practically no residue conversion during mild thermal cracking. In being able to explain this phenomenon, the model furthers the understanding of the chemistry of such short alkyl-chained polycyclic aromatic species oils and their behavior in upgrading plants and refineries.

The study of thermal cracking through carbon-type analysis helps to unravel the complex nature of petroleum feedstocks and offers an opportunity to correlate petroleum chemical structure with its behavior during physical and chemical processes. The reactivity of different visbreaker feeds including their coking behavior

can now be attributed to the structure of their constituent molecules, as quantified by NMR carbon-type analyses.

7.2 Future Work

This work focused on developing a mathematical model for visbreaking at a single reaction severity, based on principles of reaction chemistry. Future work entails developing such correlations for these feeds under different severities and then combining the information to develop a model that could predict visbreaking behavior for different oils at all reaction severities. This work is heavily dependent on the better and increased information about the kinetics of model compounds and calls for creating a library of representative model compounds based on the NMR carbon-type footprint of different heavy oils across the world. The behavior of these model compounds should be studied under thermal cracking conditions in lab to compare their relative reactivity. This comparative analysis would go a long way in understanding the chemical and physical characteristics of these heavy oils and result in their better utilization. Also NMR spectroscopy provides average carbon-type data like the average chain length and average aromatic cluster size, however it would be useful to determine the distribution and profile of parameters like chain length and cluster size, to compare different oils even better.

Bibliography

[1] Kevin Chan. *Mathematical Modeling of Thermal Conversion of Athabasca Bitumen*. Master of Science, University of Alberta, 2007.

[2] A. Sapre. Exxonmobil Resid Conversion Technologies. In *3rd Bottom of the Barrel Technology Conference & Exhibition (BBTC)*, Antwerp, October 2004.

[3] J.J. Marano. Refinery Technology Profiles-Gasification and Supporting Technologies. Technical report, National Energy Technology Laboratory, U.S. Department of Energy, June, 2003.

[4] Visbreaking. *Hydrocarbon Processing*, 75(11):144–145, 1996.

[5] G.A. van den Berg, Frans. Developments in Fuel Oil Blending. In *IASH 2000, the 7th International Conference on Stability and Handling of Liquid Fuels*, Graz, Austria, September 24-29, 2000.

[6] http://www.bp.com/. BP America History - Thermal Cracking Patent .

[7] J. G. Speight and B. Ozum. *Petroleum Refining Processes*. Marcel Dekker Inc., 2002.

[8] D.E. Allan, C.H. Martinez, C.C. Eng, and W.J. Barton. Visbreaking Gains Renewed Interest. *Chem. Eng. Prog.*, 79:85–89, 1983.

[9] M. Akbar and H. Geelen. Visbreaking Uses Soaker Drum. *Hydrocarbon Processing*, 60:81–85, 1981.

[10] J.J. McKetta. *Petroleum Processing Handbook*. Marcel Dekker Inc., 1992.

[11] T.Y. Yan. Characterization of Visbreaker Feeds. *Fuel*, 69:1062–1064, 1990.

[12] W. Olmstead and H. Freund. Thermal Conversion Kinetics of Petroleum Residua. In *AIChE Spring Meeting*, New Orleans, LA, 1998.

[13] T.Y. Yan. Symposium on Advances in Resid Upgrading. In *Division of Petroleum Chemistry Inc - American Chemical Society*, Denver, USA, April, 1987.

[14] Li Shenghua, Liu Chenguang, Que Guohe, Liang Wenjie, and Zhu Yajie. Phase Separation Behaviors and their Relations with Formation in Thermal Reaction Systems of Vacuum Residua. *Petroleum Science and Technology*, 17:693–709, 1999.

[15] I.A. Wiehe. A Phase Separation Kinetic Model for Coke Formation. *Ind. Eng. Chem. Res.*, 32:2447–2454, 1993.

[16] I.A. Wiehe. Petroleum Fouling: Causes, Tools and Mitigation Methods. In *AIChe Chicago Symposium 2006*, October 9-10, 2006.

[17] M.R. Gray. Consistency of Asphaltene Chemical Structures with Pyrolysis and Coking Behavior. *Energy and Fuels*, 17:1566–1569, 2003.

[18] Samuel Asomaning. Test Methods for Determining Asphaltene Stability in Crude Oils. *Petroleum Science and Technology*, 21:581–590, 2003.

[19] J. Singh, M.M. Kumar, A.K. Saxena, and S. Kumar. Studies on Thermal Cracking Behaviour of Residual Feedstocks in a Batch Reactor. *Chem. Eng. Sci.*, 59:4505–4515, 2004.

[20] W.R. Shu and V.N. Venkatesan. Kinetics of Thermal Visbreaking of a Cold Lake Bitumen. *J. Can. Pet. Tech.*, 23:60–64, 1984.

[21] S. Di Carlo and B. Janis. Composition and Visbreakability of Petroleum Residues. *Chem. Eng. Sci.*, 47:2695–2700, 1992.

[22] R. Krishna, Y.K. Kuchhal, G.S. Sarna, and I.D. Singh. Visbreaking Studies on Aghajari Long Residue. *Fuel*, 67:379–383, 1988.

[23] J. Singh, Y. Ram, A. Mateen, M.M. Kumar, and S. Kumar. A Four-Lump Kinetic Model for Visbreaking. *Hydrocarbon Asia*, May/Jun:32–35, 2005.

[24] J. Singh, M.M. Kumar, A.K. Saxena, and S. Kumar. Reaction Pathways and Product Yields in Mild Thermal Cracking of Vacuum Residues: A Multi-Lump Kinetic Model. *Chem. Eng. J.*, 108:239–248, 2005.

[25] K.L Kataria, R.P. Kulkarni, A.B. Pandit, J.B. Joshi, and M. Kumar. Kinetic Studies of Low Severity Visbreaking. *Ind. Eng. Chem. Res.*, 43:1373–1387, 2004.

[26] J. Castellanos, J.L. Cano, R. del Rosal, V.M. Briones, and R.L. Mancilla. Kinetic Model Predicts Visbreaker Yields. *Oil and Gas Journal*, 89(11):76–82, 1991.

[27] R.T. Morrison and R.N. Boyd. *Organic Chemistry*. Allyn and Bacon Inc., Newton, Massachusetts, 1987.

[28] F. Billaud, P. Chaverot, M. Berthelin, and E. Freund. Thermal Decomposition of Aromatics Substituted by a Long Aliphatic Chain. *Ind. Eng. Chem. Res.*, 27:1529–1536, 1988.

[29] K.L. Baxter and P.E. Savage. Pathways, Kinetics and Mechanisms for 2-Dodecyl-9,10-dihydrophenanthrene. *Ind. Eng. Chem. Res.*, 35:1517–1523, 1996.

[30] V.V Speybroeck, G.B. Marin, and M. Waroquier. Hydrocarbon Bond Dissociation Enthalpies: From Substituted Aromatics to Large Polyaromatics. *ChemPhysChem*, 7:2205–2214, 2006.

[31] F.O. Rice and K.F. Herzfeld. The Thermal Decomposition of Organic Compounds from the Standpoint of Free Radicals. VI. The Mechanism of Some Chain Reactions. *J. Am. Chem. Soc.*, 56:284, 1934.

[32] A. Kossiakoff and F.O. Rice. Thermal Decomposition of Hydrocarbons, Resonance Stabilization and Isomerization of Free Radicals. *J. Am. Chem. Soc.*, 65:590–595, 1943.

[33] B.M. Fabuss, J.O. Smith, and C.N. Satterfield. *Advances in Petroleum Chemistry and Refining*, volume 9. Wiley-InterScience, NewYork, 1964.

[34] T.I. Mizan, P.E. Savage, and B. Perry. Pyrolysis of Polycyclic Perhydroarenes. 2. 1-n-Undecylperhydronaphthalene. *Energy and Fuels*, 11:107–115, 1997.

[35] M.L. Poutsma. Free-radical Thermolysis and Hydrogenolysis of Model Hydrocarbons Relevant to Processing of Coal. *Energy and Fuels*, 4:113–131, 1990.

[36] M.R. Gray and W.C. McCaffrey. Role of Chain Reactions and Olefin Formation in Cracking, Hydroconversion, and Coking of Petroleum and Bitumen Fractions. *Energy and Fuels*, 16:756–766, 2002.

[37] Guozhong Wu, Y. Katsumura, C. Matsuura, and K. Ishigure. Comparison of Liquid-Phase and Gas-Phase Pure Thermal Cracking of n-Hexadecane. *Ind. Eng. Chem. Res.*, 35:4747–4754, 1996.

[38] M.C. Smith and P.E. Savage. Reactions of Polycyclic Alkylaromatics. 4.Hydrogenolysis Mechanisms in 1-Alkylpyrene Pyrolysis. *Energy and Fuels*, 6:195–202, 1992.

[39] R.E. Humburg and P.E. Savage. Pyrolysis of Polycyclic Perhydroarenes. 1. 9-n-Dodecylperhydroanthracene. *Ind. Eng. Chem. Res.*, 35:2096–2102, 1996.

[40] M.C. Smith and P.E. Savage. Reactions of Polycyclic Alkylaromatics. 2.Pyrolysis of 1,3-Diarylpropanes. *Energy and Fuels*, 5:146–155, 1991.

[41] S.S. Berman and AL. A. Petrov. Relative Rates of Thermal Breakdown of Individual Hydrocarbons. *Petrol. Chem. U.S.S.R.*, 23:93–98, 1983.

[42] M.C. Smith and P.E. Savage. Reactions of Polycyclic Alkylaromatics: Structure and Reactivity. *AIChE J.*, 37:1613–1624, 1991.

[43] P.E. Savage, S. Ratz, and J. Diaz. Pyrolysis of Polycyclic Perhydroarenes. 3. 1-n-Decylperhydropyrene and Structure-Reactivity Relations. *Ind. Eng. Chem. Res.*, 36:1965–1972, 1997.

[44] B.M. Fabuss, J.O. Smith, C.N. Satterfield, and R. Kafesjian. Thermal Decomposition Rates of Saturated Cyclic Hydrocarbons. *Ind. Eng. Chem. Process Des. Dev.*, 3:248, 1964.

[45] P.E. Savage, S. Ratz, and L. Tan. Pyrolysis Kinetics for Long-Chain n-Alkylcyclohexanes. *Ind. Eng. Chem. Res.*, 40:1805–1810, 2001.

[46] American Society of Testing and Materials. *Annual Book of ASTM Standards 2001, Section 5 Petroleum Products, Lubricants, and Fossil Fuels, Vol.05.06.* American Society of Testing and Materials, 2001.

[47] S. Peramanu, B.B. Pruden, and P. Rahimi. Molecular Weight and Specific Gravity Distributions for Athabasca and Cold Lake Bitumens and their Saturate, Aromatic, Resin, and Asphaltene Fractions. *Ind. Eng. Chem. Res.*, 38:3121–3130, 1999.

[48] S. Japanwala, K.H. Chung, H.D. Dettman, and M.R. Gray. Quality of Distillates from Repeated Recycle of Residue. *Energy and Fuels*, 16:477–484, 2002.

[49] M.C. Smith and P.E. Savage. Reactions of Polycyclic Alkylaromatics.1.Pathways, Kinetics and Mechanisms for 1-Dodecylpyrene Pyrolysis. *Ind. Eng. Chem. Res.*, 30:331–339, 1991.

[50] P.E. Savage and M.T. Klein. Asphaltene Reaction Pathways. 4. Pyrolysis of Tridecylcyclohexane and 2-Ethyltetralin. *Ind. Eng. Chem. Res.*, 27:1348–1356, 1988.

[51] R.J. Hooper, Battaerd, A.J. Hendrik, and D.G. Evans. Thermal Dissociation of Tetralin between 300 and 450°c. *Fuel*, 58:132–138, 1979.

[52] P.E. Savage and M.T. Klein. Asphaltene Reaction Pathways. 2. Pyrolysis of n-Pentadecylbenzene. *Ind. Eng. Chem. Res.*, 26:488–494, 1987.

[53] P.E. Savage, G.E. Jacobs, and M. Javanmardian. Autocatalysis and Aryl-Alkyl Bond Cleavage in 1-Dodecylpyrene. *Ind. Eng. Chem. Res.*, 28:645–654, 1989.

[54] K. Chan, C. Diaz-Goano, H. Dettman, and T. De Bruijn. Mathematical Modeling of Thermal Conversion of Athabasca Bitumen. In *56th Annual Technical Meeting of the Canadian International Petroleum Conference*, pages 2006–031, Calgary, AB, 13-15 June 2006.

[55] J.P. Holman. *Experimental Methods for Engineers, 3rd Edition.* McGraw-Hill, 1978.

Appendix A

List of Product Gases

A.1 Product Gases

A complete list of the product gases from visbreaking is listed in Table A.1.

Table A.1: Complete List of Product Gases

Hydrogen (H_2)
Methane (CH_4)
Ethylene (C_2H_4)
Ethane (C_2H_6)
Hydrogen Sulfide (H_2S)
Propane (C_3H_8)
Propylene (C_3H_6)
iso-Butane (i-C_4H_{10})
n-Butane (n-C_4H_{10})
trans-2-Butene (C_4H_8)
1-Butene (C_4H_8)
iso-Butene (i-C_4H_8)
cis-2-Butene (C_4H_8)
iso-Pentane (i-C_5H_{12})
3-Methyl-1-Butene (C_5H_{10})
trans-2-Pentene (C_5H_{10})
1-Pentene (C_5H_{10})
2-Methyl-1-Butene (C_5H_{10})
cis-2-Pentene (C_5H_{10})
Hexanes+ (C_6H_{14})

Appendix B

Error Analysis

B.1 Error Analysis

It is estimated that distillation analysis has an error of 0.5 absolute units, elemental analysis has an error of 0.5 absolute units, coke analysis has an error of 0.5 absolute units and carbon-type analysis has an error of 10 percent. Then, the error analysis was performed using the following method. Suppose that z = f(w, x, y,..), then the error of the function can be calculated as

$$\Delta z = \sqrt{(\frac{\partial f}{\partial w})^2(\Delta w)^2 + (\frac{\partial f}{\partial x})^2(\Delta x)^2 + (\frac{\partial f}{\partial y})^2(\Delta y)^2} \tag{B.1}$$

The quantities on the x-axis and the y-axis of the correlation plots are represented by one of these different forms:

$$y = \frac{a}{b} \tag{B.2}$$

where a = CCR content of feed or the quantity of visbreaking coke, b = feed quantity.

$$y = \frac{abc}{d} \tag{B.3}$$

where a = weight percentage carbon, b = moles of carbon-types, c = pseudo-component quantity and d = feed quantity.

$$y = \frac{a - b}{a} \tag{B.4}$$

where a = weight percentage residue in feed and b = weight percentage residue in product.

$$y = AB + C \tag{B.5}$$

where A,B and C are functions of type abc/d for different carbon-types.

$$y = \alpha_1 A + \alpha_2 B + \alpha_3 C + \alpha_4 D \tag{B.6}$$

where A, B, C, D are functions of type abc/d for different carbon-types.

The error for equations B.2, B.3, B.4, B.5 and B.6 were obtained using the Holman method [55]. The errors for equations B.2, B.3, B.4, B.5 and B.6 are shown by equations B.7, B.8, B.9, B.10 and B.11 respectively.

$$\frac{\Delta y}{y} = \sqrt{(\frac{\Delta a}{a})^2 + (\frac{\Delta b}{b})^2} \tag{B.7}$$

$$\frac{\Delta y}{y} = \sqrt{(\frac{\Delta a}{a})^2 + (\frac{\Delta b}{b})^2 + (\frac{\Delta c}{c})^2 + (\frac{\Delta d}{d})^2} \tag{B.8}$$

$$\Delta y = \frac{b}{a}\sqrt{(\frac{\Delta a}{a})^2 + (\frac{\Delta b}{b})^2} \tag{B.9}$$

$$\Delta y = AB\sqrt{(\frac{\Delta A}{A})^2 + (\frac{\Delta B}{B})^2 + (\frac{\Delta C}{AB})^2} \tag{B.10}$$

$$\Delta y = \sqrt{(\alpha_1 \Delta A)^2 + (\alpha_2 \Delta B)^2 + (\alpha_3 \Delta C)^2 + (\alpha_4 \Delta D)^2} \tag{B.11}$$

Appendix C

Sample Calculations

C.1 Sample Calculations for Athabasca Bitumen

For 100 g of Athabasca bitumen feed, weight of residue in feed = 54.6 g and weight of residue in product = 33.7 g. Percent wt carbon in RAs, RP, RA and RS in feed is 83.4, 85.1, 84.7 and 86.6 respectively. Percent wt of RAs, RP, RA and RS in feed is 19.8, 13.5, 19.2 and 2.2 respectively. Percent mol of aromatic carbon in RAs and RP is 46.5 and 42.6 respectively. The sample calculations are listed below.

1) Calculation of percent residue conversion.

$$y = \left(\frac{a-b}{a}\right) * (100) \tag{C.1}$$

where, a = weight of residue in feed and b = weight of residue in product. Substituting the values for a and b,

$$y = \left(\frac{54.6 - 33.7}{54.6}\right) * (100) \tag{C.2}$$

$$y = 38.3 \tag{C.3}$$

2) Calculation of CCR of 100 g of feed.

$$\text{Wt of aromatic carbon in RAs} = \left(\frac{19.8 * 83.4 * 46.5 * 12.011}{100 * 12.011 * 100}\right) = 7.7\text{gm} \tag{C.4}$$

$$\text{Wt of aromatic carbon in RP} = \left(\frac{13.5 * 85.1 * 42.6 * 12.011}{100 * 12.011 * 100}\right) = 4.9\text{gm} \tag{C.5}$$

$$\text{CCR content in 100 gm of feed} = (7.7 + 4.9) = 12.6\text{gm} \tag{C.6}$$

3) Calculation of carbon moles in residue fraction in 1000 g of feed

$$\text{Carbon moles in RS} = \left(\frac{2.2 * 1000 * 86.6}{100 * 12.011 * 100}\right) = 1.57 \tag{C.7}$$

$$\text{Carbon moles in RA} = \left(\frac{19.2 * 1000 * 84.7}{100 * 12.011 * 100}\right) = 13.49 \tag{C.8}$$

$$\text{Carbon moles in RP} = \left(\frac{13.5 * 1000 * 85.1}{100 * 12.011 * 100}\right) = 9.58 \tag{C.9}$$

$$\text{Carbon moles in RAs} = \left(\frac{19.8 * 1000 * 83.4}{100 * 12.011 * 100}\right) = 13.74 \tag{C.10}$$

$$\text{Total carbon moles in Resid} = (1.57 + 13.49 + 9.58 + 13.74) = 38.4 \tag{C.11}$$

4) Calculation of Residue Reactivity Index of feed

$$RRI = (A \cdot B) + C \tag{C.12}$$

where A= alkyl substituted aromatic carbon (moles), B= min (1, Alkyl chain length/5) and C= α-to-sulfides (moles). For the residue fraction in Athabasca bitumen, Alkyl chain length=4.55, percent mole of α-to-sulfides= 1.31 and percent mole of alkyl substituted aromatic carbon=9.03.

$$A = \left(\frac{9.03 * 38.4}{100}\right) = 3.47 \tag{C.13}$$

$$B = \left(\frac{4.55}{5}\right) = 0.91 \tag{C.14}$$

$$C = \left(\frac{1.31 * 38.4}{100}\right) = 0.50 \tag{C.15}$$

Substituting the values for A, B and C,

$$RRI = (3.47 \cdot 0.91) + 0.5 = 3.65 \tag{C.16}$$